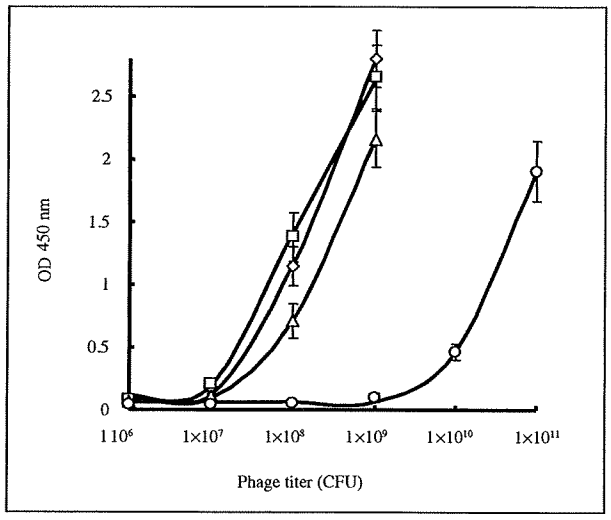

Fig. 3: Comparison of the efficiency of protein-display using pIII type phage display.
The efficiency of protein-display on pIII was assessed by phage ELISA. Proteins with different molecular weights (approximately 400–58,000 Da) were displayed on phage particle as pIII fusion proteins. This experiment was performed using the same method as Fig. 2 (n = 3). Each data value represents the mean ± S.D. □, RGDS-pIII phage; ◇, LacZ-pIII phage; △, scFv-pIII phage; ○, Importin-α-pIII phage

ated the relationship between electric charge and display efficiency using FLAG tagged ELISA (Fig. 2A). The display of positively charged SV40 NLS and HIV-1 Tat peptides were less efficient than that of the neutrally charged RGDS peptide. Generally, positively charged peptides are easy to adsorb onto various surfaces (Gaillard et al. 1999), and they repulse each other. Therefore, positively charged peptides may interfere with phage assembly in the periplasm.

Second, we examined the relationship between molecular weight and display efficiency again using FLAG tagged ELISA (Fig. 3). Because the display of positively charged sample was less efficient (Fig. 2), we used the neutrally charged proteins (pI 5.0–6.4) (MW 1.5–58 kDa) displayed on pIII to examine the influence of molecular weight on display. Phage displaying the low molecular weight RGDS peptide bound to anti-FLAG antibody at a concentration of 10^6–10^9 CFU. The higher molecular weight importin-α (58 kDa) displayed on the phage surface could not bind at the same concentration, needing 10^9–10^{11} CFU. In general, the amount of phage prepared by following the standard protocol was approximately 10^{12}–10^{13} CFU (Imai 2006). To create functional mutants using a phage library, it is desirable to use an amount of phage in excess (more than 100-fold) of the phage library (approximately 10^6–10^9 CFU). When proteins display on the phage surface efficiently, the experiment can proceed without bias. However, our result suggests that a phage library displaying high molecular weight proteins may be of low quality simply because the levels of the desired proteins are not sufficiently expressed for screening. This introduces a selection bias for those proteins that can be expressed at the proper level.

To examine the efficiency of pIII-display in greater detail, we quantified the number of molecules displayed on the phage surface by electrophoresis analysis using CsCl purified phage (Fig. 4). These results (Fig. 3, 4) demonstrate that the efficiency of RGDS peptide-display on pIII was the best (approximately 2 molecules/phage). The display efficiency decreased as the molecular weight of the target protein increased. Because the titer of all phages prepared in this experiment was determined, we suggested that the display of different molecular weight proteins did not affect the efficiency of phage-preparation (data not shown). Additionally, the proteins used in this experiment (RGDS, LacZ, scFv and importin-α) were expressed efficiently in *E. coli*. Therefore, we suggest that the efficiency with which a protein is displayed on pIII is directly related to its molecular weight.

Finally, we examined the efficiency of pVIII-display by Western blot and confirmed that it also decreased as the molecular weight increased (Fig. 5). Interestingly, this result shows that scFv (25 kDa) could be displayed on pVIII efficiently. Because the pVIII phage display system is generally believed to be limited in its application precisely by the molecular weight of displayed protein, many used it only for display of peptide libraries (Verhaert et al. 1999; Kneissel et al. 1999; Lowman 1997; Gaillard et al. 1999). However, our result suggests that the pVIII system could be applied to larger molecules. This could provide useful

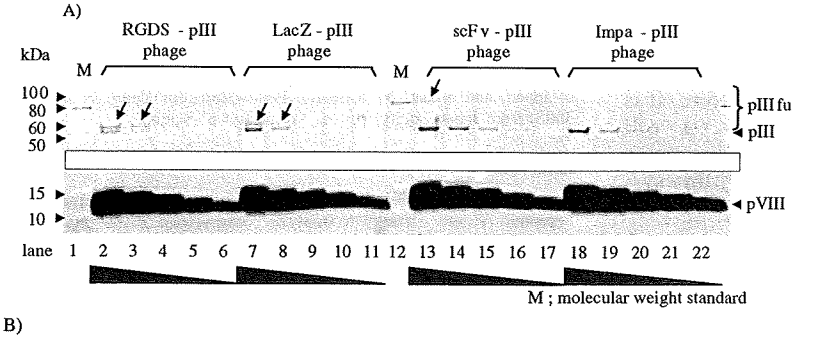

B)

	RGDS-pIII	LacZ-pIII	scFv-pIII	Impα-pIII
M.W. of displayed protein (kDa)	1.5	11	25	58
M.W. of pIII fusion protein (kDa)	52.5	62	76	109
Number of displayed proteins/phage	2.7	1.0	0.12	N.D.

N.D.; Not Detectable

Fig. 4:
Calculated quantity of pIII displayed proteins using Sypro® Ruby staining.
A) The efficiency of display on pIII was quantified using CsCl purifed phages. RGDS-pIII (lanes 2–6), LacZ-pIII (lanes 7–11), scFv-pIII (lanes 13–17) and Impα-pIII phage (lanes 18–22) were used in this experiment. Molecular weight standard was loaded in lanes 1 and 12. Starting from the left, 1×10^{13} vp, 3.3×10^{12} vp, 1.1×10^{12} vp, 3.7×10^{11} vp and 1.2×10^{11} vp were loaded. B) The number of displayed proteins per one phage particle was calculated by fluorescence image analysis. Fluorescence intensity was quantified by Typhoon image analyzer

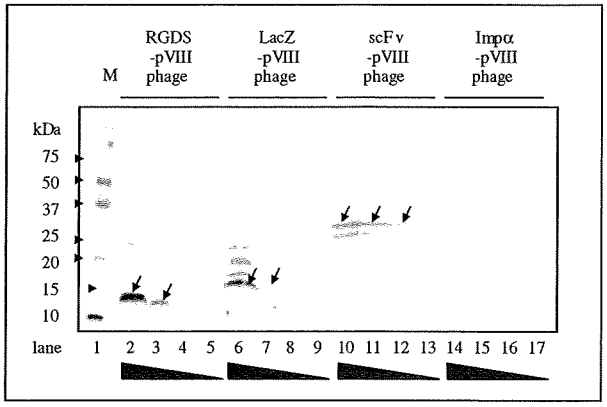

Fig. 5: Comparison of the efficiency of pVIII display protein on phage particles.
The efficiency of display on pVIII was assessed by anti-FLAG western blot. PEG-purified RGDS-pVIII (lanes 2–5), LacZ-pVIII (lanes 6–9), scFv-pVIII (lanes 10–13) and Impα-pVIII phage (lanes 14–17) were used in this experiment. Molecular weight standard was loaded in lane 1. Starting from the left, 1.5×10^{11} cfu, 5×10^{10} cfu, 1.7×10^{10} cfu and 5.5×10^{9} cfu were loaded

additional information by expanding the application of phage display systems to create various mutant proteins.
In this study, different kinds of sample peptides (SV40 NLS, HIV-1 Tat, RGDS) and proteins (RGDS, LacZ, scFv, importin-α) that could be readily expressed in *E. coli* were used as model molecules. The display of positively charged SV40 NLS and HIV-1 Tat peptides on pIII was less efficient than that of the neutrally charged RGDS peptide. When different molecular weight proteins (1.5–58 kDa) were displayed on pIII and pVIII, their display efficiencies were directly related to their molecular weights.
When comparing the efficiency of display between the four model proteins, additional factors (i.e. refolding efficiency, etc.) may account for the differences. These results show at least that the electric charge affected the efficiency of phage display and that high molecular weight proteins could not be displayed on the phage surface successfully. Recently, it was reported that improving the phagemid vector provided better efficiency of protein refolding in *E. coli* and enhanced protein display on the phage surface (Guo et al. 2003). Consequently many hope that the display efficiency of various molecules could be improved using this methodology. However, while this method improves the quality of fusion protein expression, it does not take into account the efficiency of protein assembly for the construction of phage particles. Therefore, it is still important to be able to predict the molecules that will be compatible for protein and peptide engineering using phage display by understanding the properties of this system as they were described in this report.

3. Experimental

3.1. Phagemid vectors and inserts

The pY03′-FLAG phagemid vector was modified from pCANTAB-5E (GE Healthcare Ltd.). To create this vector, the E-tag from the original vector was changed to a FLAG tag (DYKDDDDK). The pY10-FLAG phagemid vector was constructed by replacing the pIII gene in pY03′-FLAG with the pVIII gene. Genes encoding peptides (RGDS, HIV-Tat, SV40 NLS) were synthesized by Operon Biotechnologies Inc., USA. The lacZ-α gene had already been cloned into pY03′-FLAG and pY10-FLAG. The anti-KDR scFv gene was isolated from an optimized non-immune phage antibody library previously described (Imai et al. 2006). The human importin-α gene was amplified from a human bone marrow cDNA library (TAKARA Bio. Inc.). These inserts were digested and cloned into each phagemid vector.

3.2. Phage preparation

Phage was prepared by following a standard protocol. Briefly, phage particles were prepared from *Escherichia coli* (TG1 strain, Stratagene corporation) by co-infection with M13KO7 helper phage (Invitrogen Corporation). Amplified phage in culture media was roughly purified by PEG precipitation. Part of the purified phage was added to the TG1 bacteria, and the phage titer (cfu) was calculated by counting infected TG1 colonies. If necessary, additional purification using a CsCl gradient was performed as described below.

3.3. Phage ELISA

Immunoplates (Nalge Nunc International) were immobilized with anti-FLAG M2 antibody (Sigma-Aldrich Corporation) diluted to 5 μg/ml in bicarbonate buffer (Sigma-Aldrich Corporation). Plates were blocked with 2% block ace (Nakarai Tesque Inc.) for 2 h at 37 °C. Phage solution (PEG-purified) in 0.4% block ace was serially diluted and applied to the wells. After a 1 h incubation at room temperature, the binding phage was detected by anti-M13 HRP conjugate (GE Healthcare Ltd.).

3.4. Purification of phage particles under CsCl gradient

Amplified phage was purified by PEG precipitation. Phage pellets were resuspended in TBS buffer. CsCl powder (IWAI chemicals company) and additional TBS buffer were added to the phage solution up to 31%. After CsCl gradient ultracentrifugation at 400,000 × g at 5 °C for 20 h, the concentrated phage band was isolated. TBS (five volumes) was added to the purified phage and centrifuged again at 400,000 × g at 5 °C for 4 h to remove the CsCl. The obtained phage was resuspended in TBS and used for experiments.

3.5. Sypro Ruby staining

After purifying the phage under a CsCl gradient, the number of phage particles (vp/ml) was estimated from its absorbance according to the standard protocol. Serially diluted phage samples were resolved by SDS – poly acrylamide electrophoresis (SDS-PAGE). Gels were incubated in SYPRO® Ruby protein gel stain reagent (Pearce Biotechnology, Inc., USA) overnight at room temperature. After washing with wash buffer (10% methanol and 7% acetic acid) for 30 min, fluorescence was detected using the Typhoon Variable Image Analyzer (GE Healthcare Ltd.). The number of surface-displayed proteins was calculated from fluorescence intensity using ImageQuant TL software (GE Healthcare Ltd.) assuming that one phage particle contained five pIII coat proteins on its surface.

3.6. Anti-FLAG western blotting

SDS-PAGE was performed using serially diluted phage purified by PEG precipitation. Phage protein in the gel was transferred to PVDF membrane (GE Healthcare Ltd.) using the Hoefer TE 70 semi dry transfer unit (GE Healthcare Ltd.). Membranes were blocked in 4% block ace for 1 h. FLAG-tagged pVIII fusion protein was detected with anti-FLAG M2 antibody (Sigma-Aldrich Corporation) and anti-mouse IgG HRP conjugate (Sigma-Aldrich Corporation). After detection by ECL plus reagent (GE Healthcare Ltd.), its luminescence was quantitated using the LAS-3000 Lumi Imager (Fujifilm Corporation).

Acknowledgements: This study was supported in part by Grants-in-Aid for Scientific Research (No. 20015052) from the Ministry of Education, Culture, Sports, Science and Technology of Japan, by Health and Labor Sciences Research Grant from the Ministry of Health, Labor and Welfare of Japan, and in part by Research Fellowships for Young Scientists (No. 3608) from Japan Society for the Promotion of Science.

References

Bayer R, Feigenson GW (1985) Reconstitution of M13 bacteriophage coat protein. A new strategy to analyze configuration of the protein in the membrane. Biochim Biophys Acta 815: 369–379.
Chasteen L, Ayriss J, Pavlik P, Bradbury AR (2006) Eliminating helper phage from phage display. Nucleic Acids Res 34: e145.
Gaillard C, Flavin M, Woisard A, Strauss F (1999) Association of double-stranded DNA fragments into multistranded DNA structures. Biopolymers 50: 679–689.
Gourdine JP, Greenwell P, Smith-Ravin E (2005) Application of recombinant phage display antibody system in study of Codakia orbicularis gill proteins. Appl Biochem Biotechnol 125: 41–52.
Guo JQ, You SY, Li L, Zhang YZ, Huang JN, Zhang CY (2003) Construction and high-level expression of a single-chain Fv antibody fragment specific for acidic isoferritin in Escherichia coli. J Biotechnol 102: 177–189.
Imai S, Mukai Y, Nagano K, Shibata H, Sugita T, Abe Y, Nomura T, Tsutsumi Y, Kamada H, Nakagawa S, Tsunoda S (2006) Quality enhancement of the non-immune phage scFv library to isolate effective antibodies. Biol Pharm Bull 29: 1325–1330.

Keresztessy Z, Csosz E, Harsfalvi J, Csomos K, Gray J, Lightowlers RN, Lakey JH, Balajthy Z, Fesus L (2006) Phage display selection of efficient glutamine-donor substrate peptides for transglutaminase 2. Protein Sci 15: 2466–2480.

Kneissel S, Queitsch I, Petersen G, Behrsing O, Micheel B, Dubel S (1999) Epitope structures recognised by antibodies against the major coat protein (g8p) of filamentous bacteriophage fd (Inoviridae). J Mol Biol 288: 21–28.

Kuhn A (1987) Bacteriophage M13 procoat protein inserts into the plasma membrane as a loop structure. Science 238: 1413–1415.

Lowman HB (1997) Bacteriophage display and discovery of peptide leads for drug development. Annu Rev Biophys Biomol Struct 26: 401–424.

Maruta F, Parker AL, Fisher KD, Murray PG, Kerr DJ, Seymour LW (2003) Use of a phage display library to identify oligopeptides binding to the lumenal surface of polarized endothelium by ex vivo perfusion of human umbilical veins. J Drug Target 11: 53–59.

Schier R, Bye J, Apell G., McCall A, Adams GP, Malmqvist M, Weiner LM, Marks JD (1996) Isolation of high-affinity monomeric human anti-c-erbB-2 single chain Fv using affinity-driven selection. J Mol Biol 255: 28–43.

Shibata H, Yoshioka Y, Ikemizu S, Kobayashi K., Yamamoto Y, Mukai Y, Okamoto T, Taniai M, Kawamura M, Abe Y, Nakagawa S, Hayakawa T, Nagata S, Yamagata Y, Mayumi T, Kamada H, Tsutsumi Y (2004) Functionalization of tumor necrosis factor-alpha using phage display technique and PEGylation improves its antitumor therapeutic window. Clin Cancer Res 10: 8293–8300.

Sidhu SS (2001) Engineering M13 for phage display. Biomol Eng 18: 57–63.

Smith GP (1985) Filamentous fusion phage: novel expression vectors that display cloned antigens on the virion surface. Science 228: 1315–1317.

Stich N, Van Steen G, Schalkhammer T (2003) Design and peptide-based validation of phage display antibodies for proteomic biochips. Comb Chem High Throughput Screen 6: 67–78.

Takashima A, Mummert M, Kitajima T, Matsue H (2000) New technologies to prevent and treat contact hypersensitivity responses. Ann N Y Acad Sci 919: 205–213.

Verhaert RM, Van Duin J, Quax WJ (1999) Processing and functional display of the 86 kDa heterodimeric penicillin G acylase on the surface of phage fd. Biochem J 342: 415–422.

Yamamoto Y, Tsutsumi Y, Yoshioka Y, Nishibata T, Kobayashi K., Okamoto T, Mukai Y, Shimizu T, Nakagawa S, Nagata S, Mayumi T (2003) Site-specific PEGylation of a lysine-deficient TNF-alpha with full bioactivity. Nat Biotechnol 21: 546–552.

Journal of Immunological Methods 335 (2008) 71–78

Contents lists available at ScienceDirect

Journal of Immunological Methods

journal homepage: www.elsevier.com/locate/jim

Research paper

Simple and highly sensitive assay system for TNFR2-mediated soluble- and transmembrane-TNF activity

Yasuhiro Abe [a,b], Tomoaki Yoshikawa [a,c], Haruhiko Kamada [a,d], Hiroko Shibata [a,e], Tetsuya Nomura [a,b], Kyoko Minowa [a,f], Hiroyuki Kayamuro [a,b], Kazufumi Katayama [g], Hiroyuki Miyoshi [h], Yohei Mukai [a,b], Yasuo Yoshioka [a,c], Shinsaku Nakagawa [b], Shin-ichi Tsunoda [a,d,*], Yasuo Tsutsumi [a,b,d]

[a] Laboratory of Pharmaceutical Proteomics, National Institute of Biomedical Innovation, 7-6-8 Saito-Asagi, Ibaraki, Osaka 567-0085, Japan
[b] Graduate School of Pharmaceutical Sciences, Osaka University, 1-6 Yamadaoka, Suita, Osaka 565-0871, Japan
[c] The Center for Advanced Research and Education in Drug Discovery and Development, Osaka University, 1-6 Yamadaoka, Suita, Osaka 565-0871, Japan
[d] The Center for Advanced Medical Engineering and Informatics, Osaka University, 1-6 Yamadaoka, Suita, Osaka 565-0871, Japan
[e] Division of Drugs, National Institute of Health Science, 1-18-1 Kamiyoga, Setagaya-ku, Tokyo 158-8501, Japan
[f] Graduate School of Pharmaceutical Sciences, Kyoto Pharmaceutical University, Misasagi-Nakauchicho 5, Yamashina-ku, Kyoto 607-8414, Japan
[g] Allergy & Immunology Project, Tokyo Metropolitan Institute of Medical Science, 3-18-22, Honkomagome, Bunkyo-ku, Tokyo 113-8613, Japan
[h] Subteam for Manipulation of Cell Fate, BioResource Center, RIKEN, 3-1-1 Koyadai, Tsukuba, Ibaraki 305-0074, Japan

ARTICLE INFO

Article history:
Received 25 December 2007
Received in revised form 28 February 2008
Accepted 28 February 2008
Available online 26 March 2008

Keywords:
TNF
TNFR2
Fas
Chimeric receptor
Bioassay

ABSTRACT

Drugs that target tumor necrosis factor-α (TNF) are particularly important in the treatment of severe inflammatory progression in rheumatoid arthritis, Crohn's disease and psoriasis. Despite the central role of the TNF/TNF receptor (TNFR) in various disease states, there is a paucity of information concerning TNFR2 signaling. In this study, we have developed a simple and highly sensitive cell-death based assay system for analyzing TNFR2-mediated bioactivity that can be used to screen for TNFR2-selective drugs. Using a lentiviral vector, a chimeric receptor was engineered from the extracellular and transmembrane domain of human TNFR2 and the intracellular domain of mouse Fas and the recombinant protein was then expressed in TNFR1$^{-/-}$ R2$^{-/-}$ mouse preadipocytes. Our results demonstrate that this chimeric receptor is capable of inducing apoptosis by transmembrane- as well as soluble-TNF stimuli. Moreover, we found that our bioassay based on cell death phenotype had an approximately 80-fold higher sensitivity over existing bioassays. We believe our assay system will be an invaluable research tool for studying TNFR2 and for screening TNFR2-targeted drugs.

1. Introduction

Tumor necrosis factor-α (TNF) is a pleiotropic cytokine that regulates various biological processes such as host defense, inflammation, autoimmunity, apoptosis and tumor cell death through the TNF-receptor 1 (TNFR1) and receptor 2 (TNFR2) (Wajant et al., 2003). TNF/TNFR interaction is considered to be an attractive target for the treatment of refractory diseases, including autoimmune disease and malignant tumors (Aggarwal, 2003; Szlosarek and Balkwill, 2003). In rheumatoid arthritis, for example, biological anti-TNF agents, such as Infliximab and Adalimumab, rapidly reduce signs and symptoms of joint inflammation (Feldmann and Maini, 2003). However, anti-TNF drugs used to treat inflammatory disorders have been reported to increase the risk of infection, in accordance with animal studies (Brown et al., 2002; Nathan et al., 2006).

* Corresponding author. Laboratory of Pharmaceutical Proteomics, National Institute of Biomedical Innovation, 7-6-8 Saito-Asagi, Ibaraki, Osaka 567-0085, Japan. Tel.: +81 72 641 9811x2327; fax: +81 72 641 9817.
E-mail address: tsunoda@nibio.go.jp (S. Tsunoda).

0022-1759/$ – see front matter © 2008 Elsevier B.V. All rights reserved.
doi:10.1016/j.jim.2008.02.019

A thorough understanding of the biology of the TNF/TNFR system is a prerequisite to the safe and effective development of anti-TNF therapeutics. In particular, several factors and mechanisms hypothesized to be involved in the side effects elicited by anti-TNF drugs need to be tested (Curtis et al., 2007; Jacobs et al., 2007; Schneeweiss et al., 2007). These include the differential power of the drugs to neutralize TNF bioavailability and the differential inhibition of TNF signaling events. Despite extensive studies on the molecular biology of TNF/TNFR1 signaling (Micheau and Tschopp, 2003) the functions of TNFR2 are poorly understood. There is an increasing need for a comprehensive understanding of TNF/TNFR2 biology, particularly in terms of the development of TNFR-selective drugs.

In this context, we have used a novel phage-display based screening system (Yamamoto et al., 2003; Shibata et al., 2004, 2008) to develop structural mutants of TNF to help clarify the biology of TNF/TNFR2 interactions. These TNF variants, which exert TNFR2-mediated agonistic or antagonistic activity, might be extremely valuable for elucidating structure-activity relationships between TNF and TNFR2. So far, in order to evaluate the bioactivity of TNF through TNFR2, many researchers have used the TNFR2 over-expressing cell lines (Heller et al., 1992; Weiss et al., 1998), such as rat/mouse T hybridomas transfected with human TNFR2 (PC60-hR2) (Vandenabeele et al., 1992). The PC60-hR2 assay is based on granulocyte macrophage colony-stimulating factor (GM-CSF) secretion mediated by TNF/TNFR2 stimuli. The GM-CSF secretion level is quantified by proliferation of GM-CSF-dependent cell lines or by ELISA. However, this two-step assay system is complicated and the screening process is highly laborious. Thus, there are increasing demands for the development of a simple, highly sensitive screening system that is TNFR2-selective.

In the present study, we developed a simple but highly sensitive cell death-based assay system for evaluating TNFR2-mediated activity. We constructed a lentiviral vector expressing a chimeric receptor derived from the extracellular (EC) and transmembrane (TM) domain of human TNFR2 (hTNFR2) and the intracellular (IC) domain of mouse Fas (mFas). Additionally, to eliminate the influence of the endogenous TNFR1, the chimeric receptor was expressed on TNFR1$^{-/-}$R2$^{-/-}$ preadipocytes (Xu et al., 1999). We found that hTNFR2/mFas-expressing preadipocyte (hTNFR2/mFas-PA) showed about 80-times higher sensitivity after treatment with soluble-TNF and over the conventional method. Furthermore, hTNFR2/mFas-PA could detect not only transmembrane TNF- (tmTNF) but also soluble TNF-activity. The technology described herein will be highly useful both as an assay system for various TNF variants *via* TNFR2 and also as a cell-based drug discovery system for TNFR2 agonists/antagonists.

2. Materials and methods

2.1. Cell culture

TNFR1$^{-/-}$R2$^{-/-}$, TNFR1$^{-/-}$, and wild-type (wt) preadipocytes established from day 16–17 mouse embryos were generously provided by Dr. Hotamisligil (Harvard School of Public Health, Boston MA). Preadipocytes, 293T cells and HeLaP4 cells were cultured in Dulbecco's modified Eagle's medium (DMEM; Sigma-Aldrich, Inc., Tokyo, Japan) with 10% bovine fetal serum (FBS) and 1% antibiotic cocktail (penicillin 10,000 u/ml, streptomycin 10 mg/ml, and amphotericin B 25 μg/ml; Nacalai Tesque, Kyoto, Japan). The rat/mouse T hybridomas PC60-hR2 cells (hTNFR2 transfected PC60 cells) were generously provided by Dr. Vandenabeele (University of Gent, Belgium) and cultured in RPMI 1640 (Sigma-Aldrich, Inc.) with 10% FBS, 1 mM sodium pyrubate, 5×10^{-5} M 2-ME, 3 μg/ml puromycin (Wako Pure Chemical Industries, Osaka, Japan), and 1% antibiotic cocktail. TNFR1$^{-/-}$R2$^{-/-}$ mouse macrophages were generously provided by Dr. Aggarwal (University of Texas MD Anderson Cancer Center, Houston, TX), and cultured in RPMI 1640 with 10% FBS and 1% antibiotic cocktail.

2.2. Construction of self-inactivating (SIN) lentiviral vector

Vectors were constructed using standard cloning procedures. A DNA fragment encoding the EC and TM parts of hTNFR2 was amplified by polymerase chain reaction (PCR) from human peripheral blood lymphocyte cDNA with the following primer pairs: forward primer (5′-GAT TAC GCC AAG CTT GTC GAC CAC CAT GGC GCC CGT CGC CGT CTG GGC CGC GCT GGC CGT CGG ACT GGA G-3′) containing a SalI site at the 5′-end and a reverse primer (5′-CAC CTT GGC TTC TCT CTG CTT TCG AAG GGG CTT CTT TTT CAC CTG GGT CA-3′) containing a Csp45I site. The resulting amplified fragment was subcloned into pCR-Blunt II-TOPO (Invitrogen Corp., Carlsbad, CA) to generate pCR-Blunt-hTNFR2. A fragment encoding the IC domain of mFas was amplified by PCR from mouse spleen cDNA with the following primer pair: forward primer (5′-AAT TCC ACT TGT ATT TAT ACT TCG AAA GTA CCG GAA AAG A-3′) containing a Csp45I site and a reverse primer (5′-GTC ATC CTT GTA GTC TGC GGC CGC TCA CTC CAG ACA TTG TCC TTC ATT TTC ATT TCC A-3′) containing a NotI site at the 5′-end. The mFas DNA fragment was subcloned into pCR-Blunt-hTNFR2 between the Csp45I and NotI sites to combine the EC and TM domains of hTNFR2 to the IC domains of mFas, generating pCR-Blunt-hTNFR2/mFas (Fig. 1A). Then the hTNFR2/mFas DNA fragment was cloned between the XhoI and NotI sites of SIN lentiviral vector construct, which contains the blasticidin (Bsd) resistance gene, generating CSII-CMV-hTNFR2/mFas-IRES2-Bsd (Fig. 1B). For construct tmTNF, a DNA fragment encoding non-cleavable human tmTNF h(tmTNFΔ1-12), generated by deleting amino acids 1–12 in the N-terminal part of hTNF, was amplified by PCR from hTNF cDNA with following primer pair: forward primer (5′-AGT GAT CGG CCC CCA GAG GGA AGC TTA GAT CTC TCT CTA ATC AGC CCT CTG GCC CAG GCA GTA GCC CAT GTT GTA GCA AAC CCT CAA G-3′) and reverse primer (5′-GGT TGG ATG TTC GTC CTC CGC GGC CGC CTA ACT AGT TCA CAG GGC AAT GAT CCC AAA GTA GAC CTG-3′) and cloned into the pY03′ vector. Then tmTNFΔ1–12 DNA fragment was cloned between the SalI and XhoI sites of the SIN vector construct, generating CSII-EF-tmTNF-IRES-GFP.

2.3. Preparation of lentiviral vectors

The method used to prepare the lentiviral vector has been described previously (Miyoshi et al., 1999; Katayama et al.,

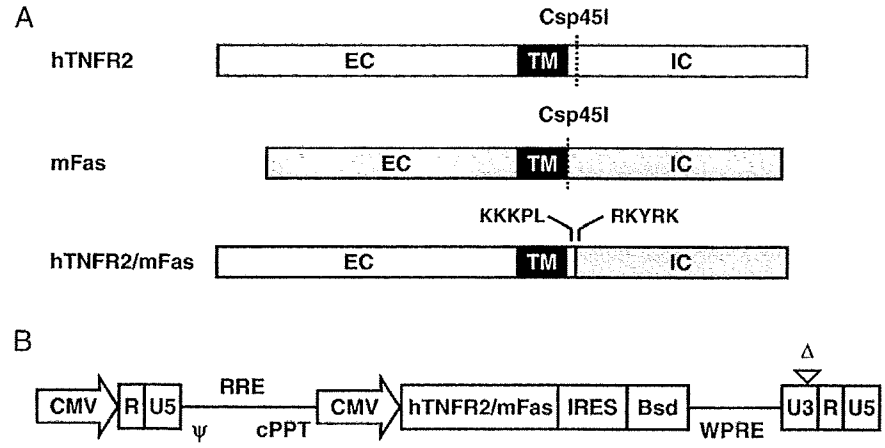

Fig. 1. Construction of hTNFR2/mFas chimeric receptor gene and vector. (A) The cDNA structures of hTNFR2, mFas and fusion genes (hTNFR2/mFas) are shown. EC: extracellular domain, TM: transmembrane domain, IC: Intracellular domain. (B) Schematic representation of self-inactivating (SIN) LV plasmid (CSII-CMV-hTNFR2/mFas-IRES-Bsd). CMV, cytomegalovirus promoter; ψ: packaging signal; RRE, rev responsive element; cPPT, central polypurine tract; IRES, Encephalomyocarditis virus internal ribosomal entry site; Bsd, Blasticidin; WPRE, woodchuck hepatitis virus posttranscriptional regulatory element. Δ: deleting 133 bp in the U3 region of the 3′ long terminal repeat.

2004). In brief, 293T cells were transfected by the calcium phosphate method with three plasmids: packaging construct (pCAG-HIVgp), VSV-G and Rev expressing construct (pCMV-VSV-G-RSV-Rev) and SIN vector construct (CSII-CMV-TNFR2/Fas-IRES2-Bsd or CSII-EF-tmTNF-IRES-GFP). Two days after transfection, the conditioned medium was collected and the virus was concentrated by ultracentrifugation at 50,000 × *g* for 2 h at 20 °C. The pelleted virus was resuspended in Hanks' balanced salt solution (GIBCO BRL, Paisley, UK). Vector titers were determined by measuring the infectivity of HeLaP4 cells with serial dilutions of vector stocks using flow cytometric analysis (FCM) for hTNFR2/mFas- or GFP-positive cells.

2.4. Preparation of hTNFR2/mFas- or tmTNF-expressing cell culture

To prepare the hTNFR2/mFas- or tmTNF-expressing cell culture, $TNFR1^{-/-}R2^{-/-}$ preadipocytes or $TNFR1^{-/-}R2^{-/-}$ macrophages were infected with each lentiviral vector at a multiplicity of infection (MOI) of 100. Stable hTNFR2/mFas-transfectants were selected for growth in culture medium containing 8 μg/ml Bsd (Invitrogen Corp.) for 1 week. Expression of hTNFR2/mFas chimeric receptor on Bsd-resistant cells was detected by staining with biotinylated anti-hTNFR2 antibody (BD Biosciences, Franklin Lakes, NJ) at 0.5 μg/5×10^5 cells for 30 min at 4 °C. Subsequently, the cells were washed and stained with streptavidin-PE conjugate (BD Biosciences). The cell suspension was centrifuged at 800 × *g*, washed with PBS, centrifuged again, and then re-suspended in 500 μl of 0.4% paraformaldehyde. Fluorescence was analyzed on a FACS Vantage flow cytometer, and data were analyzed using CellQuest software (both BD Biosciences). The hTNFR2/mFas-positive cell cultures were used in subsequent experiments as hTNFR2/mFas-PA cells. For preparation of tmTNF-expressing $TNFR1^{-/-}R2^{-/-}$ macrophages (tmTNF-Mφ), IRES-driven GFP positive cells were sorted by FACSAria (BD Biosciences).

2.5. Cytotoxicity assays

Cells were seeded on 96-well micro titer plates at a density of 1.5×10^4 cells/well in culture medium. Serial dilutions of mouse or human TNF (mTNF or hTNF; Peprotech, Rocky Hill, NJ), anti-mFas antibody (clone Jo2; BD Biosciences), or paraformaldehyde-fixed tmTNF-Mφ were prepared with DMEM containing 1 μg/ml cycloheximide, and added to each well. After 48 h incubation, the cell viability was measured by WST-8 assay kit (Nacalai Tesque) according to the manufacturer's instructions. The assay is based on cleavage of the tetrazolium salt WST-8 to formazan by cellular mitochondrial dehydrogenase.

2.6. Induction of GM-CSF secretion on PC60-hR2

5×10^4 of PC60-hR2 cells were seeded on a 96 well plate and then exposed to a serial dilution of hTNF in the presence of IL-1β (2 ng/ml). After 24 h incubation, hTNFR2-mediated GM-CSF secretion on PC60-hR2 cells was quantified by ELISA kit according to the manufacturer's protocol (R&D Systems, Minneapolis, MN).

2.7. Immunoprecipitation and western blotting

For immunoprecipitation we used FLAG-TNF (a FLAG-tag fusion protein of hTNF), which was generated in *E. coli* and purified in our laboratory. The protocol for the expression and purification of recombinant proteins has been described previously (Yamamoto et al., 2003). 1×10^7 hTNFR2/mFas-PA cells were treated with or without 100 ng/ml of FLAG-TNF for 30 min at 37 °C. Cells were then harvested and lysed in 1 ml of lysis buffer (50 mM Tris HCl, pH 7.4, 150 mM NaCl, 1% Triton X-100, 1 mM EDTA and protease inhibitor cocktail; Sigma-Aldrich Inc.) and gently rocked at 4 °C for 30 min. Cell debris was removed by centrifugation at 10,000 ×*g* for 30 min. The resulting supernatant was immunoprecipitated with anti-FLAG-M2 affinity beads (Sigma, St.Louis, MO) for 4 h at 4 °C. Immune complexes bound to the beads were washed three

times with 500 μl of lysis buffer and eluted with 3×FLAG peptide at a concentration of 150 ng/ml. Collected proteins were resolved on 10–20% SDS-PAGE gels and transferred to polyvinylidene fluoride membranes (Millipore Corp., Billerica, MA) by electroblotting. Western blot analyses were performed with biotinylated anti-hTNFR2 antibody (R&D systems) or anti-FADD (Fas-associated death domain protein) antibody (H-181; Santa Cruz Biotechnology Inc., Santa Cruz, CA). Bound primary antibodies were visualized with horseradish peroxidase-conjugated streptavidin or goat–anti-rabbit-IgG (Jackson Immunoresearch Lab., West Grove, PA) respectively, and ECL plus western blotting detection reagents (GE Healthcare, Buckinghamshire, UK). A LAS 3000 image analyzer (Fujifilm, Tokyo, Japan) was used for the observation of chemiluminescence.

3. Results

3.1. Fas- but not TNFR-mediates induction of cell-death in $TNFR1^{-/-}R2^{-/-}$ preadipocytes

Initially, we established a cell line that could be used to evaluate TNFR2-specific bioactivity by means of the chimeric receptor (hTNFR2/mFas) strategy. The parental cell line must

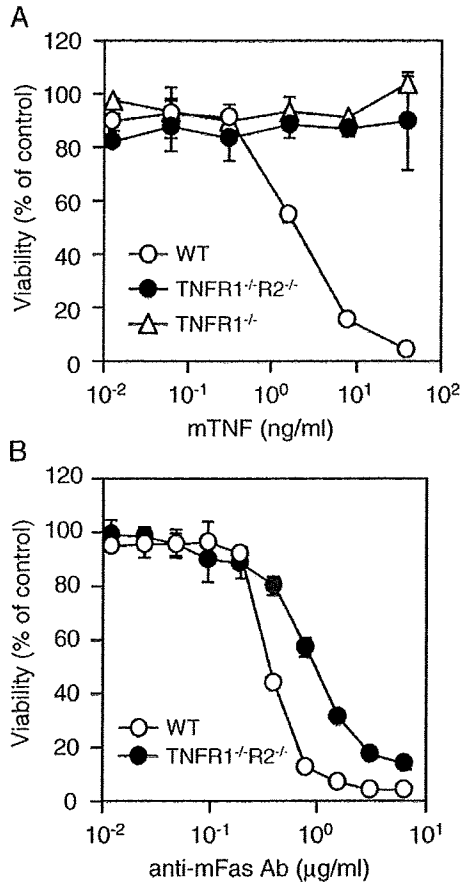

Fig. 2. Fas, but not TNFR2, induced cell death in preadipocytes. WT, $TNFR1^{-/-}R2^{-/-}$ and $TNFR1^{-/-}$ cells were treated with serial dilutions of (A) mTNF or (B) anti-mFas Ab. Cell viability was determined using the WST-8 Assay. Each data point represents the mean±SD of triplicate wells.

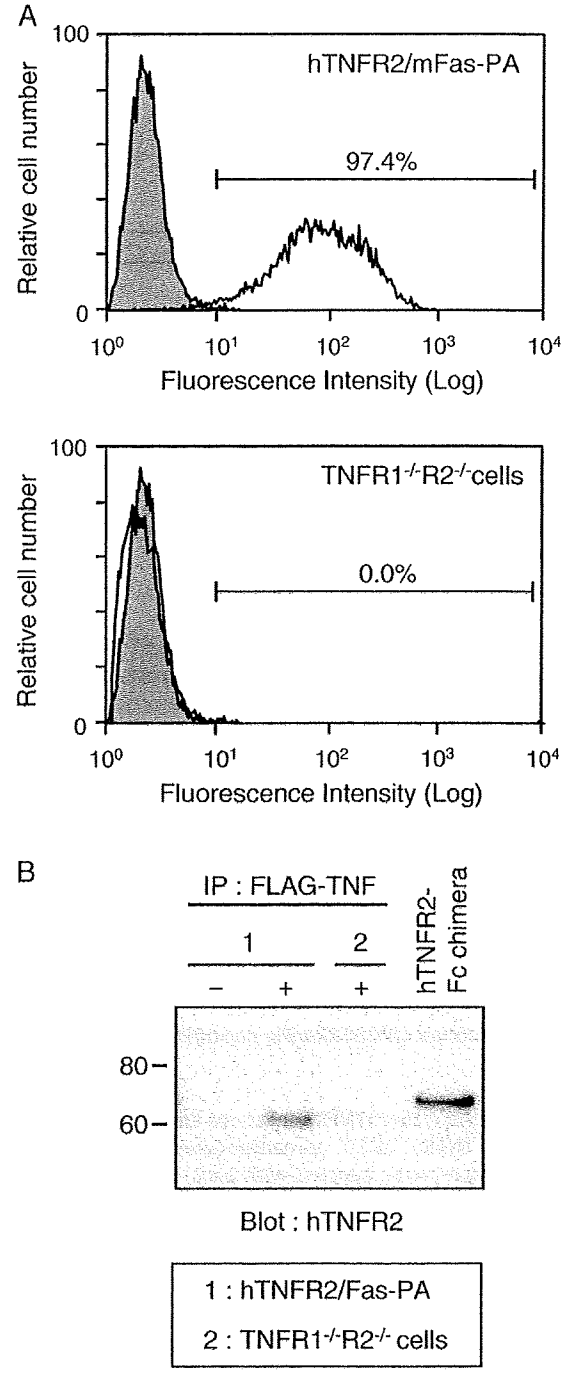

Fig. 3. Expression of hTNF2/mFas chimeric receptor on transfectants. (A) Expression of the chimeric receptor on hTNFR2/mFas-PA (upper panel) or parental $TNFR1^{-/-}R2^{-/-}$ cells (lower panel) was analyzed by flow cytometry using hTNFR2-specific antibody (open histograms) or isotype control antibody (shaded histograms). (B) hTNFR2/mFas-PA or $TNFR1^{-/-}R2^{-/-}$ cells were treated (+) with FLAG-TNF; (−) denotes untreated control cells. Immunoprecipitation was performed with anti-FLAG antibody M2-conjugated beads. After extensive washing, the immunocomplexes were eluted with 3×FLAG peptide. Eluted proteins were resolved on 10–20% SDS-PAGE gels and the presence of hTNFR2/mFas in the complex was detected by western blot using anti-hTNFR2 antibody.

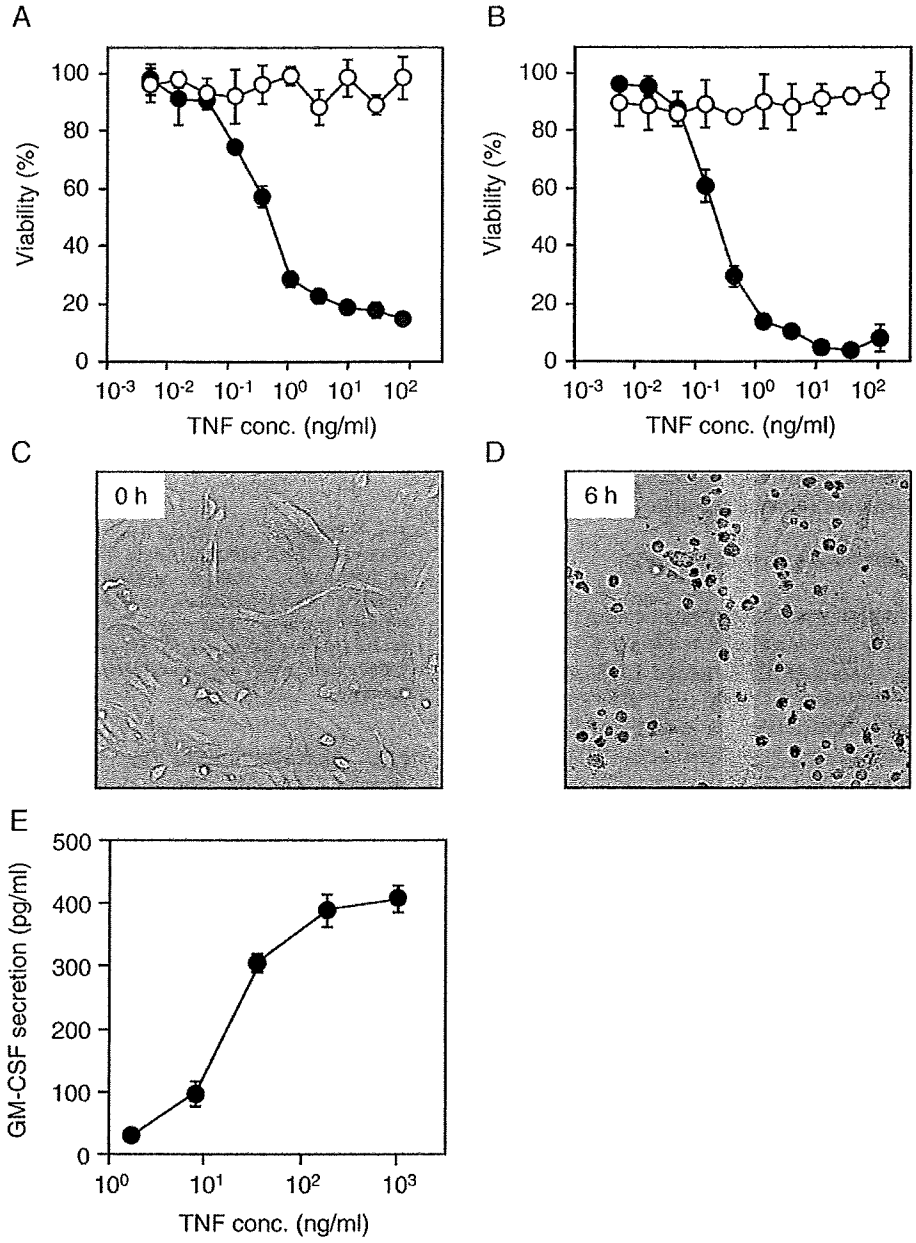

Fig. 4. Induction of strong cell death on hTNFR2/mFas-PA by soluble hTNF. hTNFR2/mFas-PA (●) and parental TNFR1$^{-/-}$R2$^{-/-}$ (○) cells were treated with serial dilutions of hTNF in the presence of cycloheximide (1 μg/ml). After (A) 24 h and (B) 48 h, the cell viability was measured using the WST-8 Assay. Data from the WST-8 assay represents the mean and SDs of triplicate assays. Similar results were obtained in three independent experiments. (C) Untreated or (D) hTNF-treated (10 ng/ml) hTNFR2/mFas-PA cells were incubated for 6 h, and were assessed by light microscopy. (E) PC60-hR2 cells were incubated in the presence of a serial dilution of hTNF and IL-1β (2 ng/ml). After 24 h, induction of GM-CSF was determined by ELISA. Each data point represents the mean±SD of triplicate measurements.

possess both Fas-sensitivity and TNF-resistance. Thus, we selected TNFR1$^{-/-}$R2$^{-/-}$ preadipocytes as the parental cell line and then examined the susceptibility of this cell line against TNFR1- and Fas-induced cell death. TNFR1$^{-/-}$R2$^{-/-}$ preadipocytes were resistant to TNF-induced cell death, while WT preadipocytes, which co-express both TNFR1 and TNFR2, were killed by mTNF-treatment in a dose-dependent manner (Fig. 2A). TNFR1$^{-/-}$ preadipocytes were also resistant to TNF-induced cell death. Thus, TNF-mediated cell death is presumably due to TNFR1-stimuli in accordance with previous reports (Vandenabeele et al., 1995; Ashkenazi and Dixit, 1998; Devin et al., 2000). Anti-Fas antibody treatment induced cell death for both WT, R1$^{-/-}$ and TNFR1$^{-/-}$R2$^{-/-}$ preadipocytes (Fig. 2B). Based on these results, we therefore selected TNFR1$^{-/-}$R2$^{-/-}$ preadipocytes for constructing an hTNFR2/mFas-expressing cell line.

3.2. hTNFR2-expression analysis of LV-hTNFR2/mFas-Bsd infected Bsd-resistant cells

Using the LV technique followed by Bsd selection, we established transfectants that stably expressed hTNFR2/mFas chimeric receptor in which the EC and TM portion of hTNFR2 (amino acids 1–292) was fused to the IC region of mFas (amino acids 187–328) (Figs. 1A and B). FCM analysis revealed that almost 95% of Bsd-resistant cells expressed the EC domain of hTNFR2 (Fig. 3A). To determine whether hTNFR2/mFas retained binding activity against hTNF, we next performed immunoprecipitation and western blot analysis (Fig. 3B). These analyses showed that FLAG-TNFs were immunoprecipitated and eluted with hTNFR2/mFas from LV-transfected and Bsd-resistant cells, but not from parental TNFR1$^{-/-}$R2$^{-/-}$ preadipocytes and untreated cells. Thus, we succeeded in constructing hTNFR2/mFas expressing TNFR1$^{-/-}$ R2$^{-/-}$ preadipocytes that retained the ability to bind hTNF.

3.3. Induction of apoptosis on hTNFR2/mFas-PA

To examine whether the death signal could be transduced by stimulating the chimeric receptors, we evaluated the cell viability of soluble hTNF-treated hTNFR2/mFas-PA. As anticipated, addition of hTNF to hTNFR2/mFas-PA induced a strong cytotoxic effect 24 and 48 h later, whereas no cell death was detected using parental TNFR1$^{-/-}$R2$^{-/-}$ preadipocytes (Figs. 4A and B). After 48 h, more than 90% of hTNFR2/mFas-PA cells were killed by hTNF at a concentration of 4 ng/ml, resulting in a median effective concentration (EC50) of 250 pg/ml. The images in Figs. 4C and D show that hTNFR2/mFas-PA cells underwent clear morphological changes, indicating apoptosis by hTNF stimuli. Additionally, PC60-hR2 cells were tested for hTNFR2-mediated GM-CSF secretion (Fig. 4E). The concentration required to induce 50% of maximal secretion of GM-CSF obtained with hTNF (EC50) was approximately 20 ng/ml. Importantly, our bioassay based on cell death phenotype displayed a ~80-fold higher level of sensitivity over conventional methodologies. Moreover, tmTNF (Fig. 5) and anti-TNFR2 agonistic antibody (data not shown) induced hTNFR2/mFas-PA cell death.

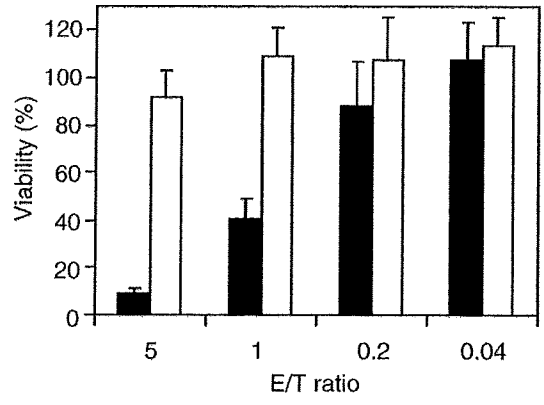

Fig. 5. hTNFR2/mFas-PA cells could be induced cell death by tmTNF. hTNFR2/mFas-PA cells were co-incubated with paraformaldehyde-fixed tmTNF-Mϕ (filled bars) or TNFR1$^{-/-}$R2$^{-/-}$ Mϕ (open bars) at an effector/target (E/T) ratio of 5:1, 1:1, 0.2:1 and 0.4:1 in the presence of cycloheximide (1 μg/ml). After 48 h, cell viability was measured by WST-8 Assay. Each data point represents the mean±SD of triplicate measurements.

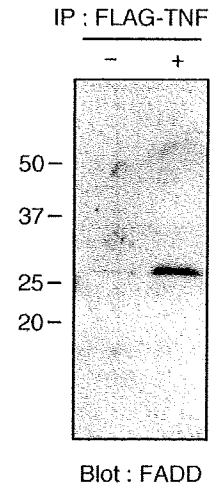

Fig. 6. Recruitment of FADD to the hTNFR2/mFas chimeric receptor in response to hTNF. hTNFR2/mFas-PA or TNFR1$^{-/-}$R2$^{-/-}$ cells were treated (+) with FLAG-TNF; (–) denotes untreated cells. Immunoprecipitation was performed with anti-FLAG antibody M2-conjugated beads. After extensive washing, immunocomplexes were eluted with 3×FLAG peptide. The eluted proteins were resolved on 10–20% SDS-PAGE gels and the presence of hTNFR2/mFas in the complex was detected by western blot using anti-FADD Antibody.

3.4. Recruitment of FADD to the hTNFR2/mFas chimeric receptor

Recent studies indicate that some TNFR family members, including Fas, self-associate as trimers prior to ligand binding. Activation of the pre-associated receptors is triggered by ligand-induced rearrangement of the assembled trimers (Algeciras-Schimnich et al., 2002). We speculated that the first reaction after ligand-induced oligomerization of hTNFR2/mFas might be the recruitment of FADD, leading to caspase-8 activation. To investigate the composition of the ligand-hTNFR2/mFas signaling complex, we treated hTNFR2/mFas-PA cells with FLAG-tagged hTNF and affinity purified the receptor complex using anti-FLAG antibody-conjugated beads, followed by western blot analysis with antibody against FADD. As expected, FADD was immunoprecipitated with hTNFR2/mFas on hTNF-treated hTNFR2/mFas-PA (Fig. 6). In similar experiments, we could not detect TRADD, which is recruited to TNFR1 in a ligand-dependent process (data not shown). It has been reported that, in contrast to TNFR1, Fas does not interact with TRADD but directly recruits FADD, leading to efficient cell death (Stanger et al., 1995; Dempsey et al., 2003). Because hTNFR2/mFas interacts with FADD, our hTNFR2/mFas-PA cell-based assay system will be useful for evaluating hTNF activity specifically *via* hTNFR2.

4. Discussion

Here, we developed a hTNFR2/mFas-PA cell-based assay system in order to investigate hTNF activity through hTNFR2. The assay is simple to perform and can detect hTNF-mediated hTNFR2 activity with high sensitivity. Because the hTNFR2/

mFas-PA system was engineered in TNFR1$^{-/-}$R2$^{-/-}$ preadipocytes, we were able to analyze hTNF-mediated hTNFR2 activity without affecting TNFR1-related apoptosis. Moreover, not only tmTNF- but also soluble TNF-mediated hTNFR2 activity was detectable using the hTNFR2/mFas-PA cell system.

In our system, hTNFR2-mediated cytotoxic activity on hTNFR2/mFas-PA cells was quantitatively determined using the WST-8 assay. Alternative methods, such as the MTT assay or Methylene Blue assay, are also capable of detecting cytotoxicity. Using the WST-8 assay, hTNFR2-mediated cytotoxic activity was readily detected 24 h after hTNF treatment (Fig. 4A), although a stronger signal was generated with a longer incubation time (48 h; Fig. 4B). Therefore, 48 h-treatment might be more appropriate for evaluating the activity of a low dose of hTNF or when analyzing an activity-weakened mutant TNF. Furthermore, if you evaluate in the absence of CHX, it may be desirable to alter the cell numbers from 1.5 to 1.0×10^4 cells/well. Previously, a similar assay system to the one described in this report was developed by Heidenreich et al. based on murine TNFR1$^{-/-}$R2$^{-/-}$ cells, which heterogenetically expressed human Fas conjugated with hTNFR2 (termed MF-R2-Fas cells) (Krippner-Heidenreich et al., 2002). However, there are some important differences between the MF-R2-Fas cells and the cell line used in our assay system (hTNFR2/mFas-PA), such as detachability. Surprisingly, unlike MF-R2-Fas cells, hTNFR2/mFas-PA cells can detect tmTNF-mediated activity as well as soluble TNF activity. Currently, the reason for this difference is unclear, although it may be caused by heterogeneity of the Fas domain. Indeed, the genetic homology between murine Fas and human Fas in IC domain is approximately 50%. Additionally, other factors may account for the observed differences between the two assay systems, such as expression level of the chimeric receptor. At any event, our results suggest that hTNFR2/mFas-PA cells will be useful in providing the basis for a highly sensitive assay system for analyzing hTNFR2 activity mediated by both soluble TNF and tmTNF. We are currently attempting to generate a TNFR2-selective mutant TNF using this assay system and a phage display system for TNF-therapy or anti-TNF therapy (unpublished data). We chose to use hTNFR2/mFas-PA cells in the screening process for a TNFR2-selective mutant TNF because this cell line is sensitive against not only purified TNF but also culture supernatants of TNF-transfected *E. coli* (crude samples). Therefore, our simple and sensitive bioassay enables high-throughput screening for TNFR2-selective mutant TNFs. The TNFR2-selective mutant will make it possible to perform a structure-function study of TNF/TNFR at any stage of function.

With the success of the human genome project, the focus of life science research has shifted to functional and structural analyses of proteins, such as disease proteomics (Oh et al., 2004; Gilchrist et al., 2006). Thus, there is increasing expectation on drug discovery/development based on the information from genomics or proteomics research, structural biology studies, or receptor-ligand interaction analyses. In particular, the therapeutic application of bioactive proteins, such as cytokines and the newly identified ligand proteins, is eagerly awaited (Gollob et al., 2003; Ansell et al., 2006). Surprisingly, however, these ligand proteins display multiple functions, which has severely limited their clinical application (Margolin et al., 1994; Eskander et al., 1997). Because the reason behind this limitation is that these ligand proteins stimulate different signal transduction pathways via multiple (two or more) receptors, the discovery of receptor-specific agonistic or antagonistic drugs is keenly awaited. Our assay system using a chimeric receptor strategy is applicable to other cytokines and thereby provides a new avenue for identifying receptor-specific agonists or antagonists. We fully anticipate that our novel technology will accelerate the development of TNFR2-related therapeutic molecules as well as acting as a research tool for studying the biology of TNFR2.

Acknowledgements

This study was supported in part by Grants-in-Aid for Scientific Research (No. 18015055, 17689008) from the Ministry of Education, Culture, Sports, Science and Technology of Japan, in part by Health Labor Sciences Research Grant from the Ministry of Health, Labor and Welfare of Japan, in part by Health Sciences Research Grants for Research on Health Sciences focusing on Drug Innovation from the Japan Health Sciences Foundation, and in part by JSPS Research Fellowships for Young Scientists from the Japan Society for the Promotion of Science.

References

Aggarwal, B.B., 2003. Signalling pathways of the TNF superfamily: a double-edged sword. Nat. Rev. Immunol. 3, 745.

Algeciras-Schimnich, A., Shen, L., Barnhart, B.C., Murmann, A.E., Burkhardt, J.K., Peter, M.E., 2002. Molecular ordering of the initial signaling events of CD95. Mol. Cell Biol. 22, 207.

Ansell, S.M., Geyer, S.M., Maurer, M.J., Kurtin, P.J., Micallef, I.N., Stella, P., Etzell, P., Novak, A.J., Erlichman, C., Witzig, T.E., 2006. Randomized phase II study of interleukin-12 in combination with rituximab in previously treated non-Hodgkin's lymphoma patients. Clin. Cancer Res. 12, 6056.

Ashkenazi, A., Dixit, V.M., 1998. Death receptors: signaling and modulation. Science 281, 1305.

Brown, S.L., Greene, M.H., Gershon, S.K., Edwards, E.T., Braun, M.M., 2002. Tumor necrosis factor antagonist therapy and lymphoma development: twenty-six cases reported to the Food and Drug Administration. Arthritis Rheum. 46, 3151.

Curtis, J.R., Patkar, N., Xie, A., Martin, C., Allison, J.J., Saag, M., Shatin, D., Saag, K.G., 2007. Risk of serious bacterial infections among rheumatoid arthritis patients exposed to tumor necrosis factor alpha antagonists. Arthritis Rheum. 56, 1125.

Dempsey, P.W., Doyle, S.E., He, J.Q., Cheng, G., 2003. The signaling adaptors and pathways activated by TNF superfamily. Cytokine Growth Factor Rev. 14, 193.

Devin, A., Cook, A., Lin, Y., Rodriguez, Y., Kelliher, M., Liu, Z., 2000. The distinct roles of TRAF2 and RIP in IKK activation by TNF-R1: TRAF2 recruits IKK to TNF-R1 while RIP mediates IKK activation. Immunity 12, 419.

Eskander, E.D., Harvey, H.A., Givant, E., Lipton, A., 1997. Phase I study combining tumor necrosis factor with interferon-alpha and interleukin-2. Am. J. Clin. Oncol. 20, 511.

Feldmann, M., Maini, R.N., 2003. Lasker Clinical Medical Research Award. TNF defined as a therapeutic target for rheumatoid arthritis and other autoimmune diseases. Nat. Med. 9, 1245.

Gilchrist, A., Au, C.E., Hiding, J., Bell, A.W., Fernandez-Rodriguez, J., Lesimple, S., Nagaya, H., Roy, L., Gosline, S.J., Hallett, M., Paiement, J., Kearney, R.E., Nilsson, T., Bergeron, J.J., 2006. Quantitative proteomics analysis of the secretory pathway. Cell 127, 1265.

Gollob, J.A., Veenstra, K.G., Parker, R.A., Mier, J.W., McDermott, D.F., Clancy, D., Tutin, L., Koon, H., Atkins, M.B., 2003. Phase I trial of concurrent twice-weekly recombinant human interleukin-12 plus low-dose IL-2 in patients with melanoma or renal cell carcinoma. J. Clin. Oncol. 21, 2564.

Heller, R.A., Song, K., Fan, N., Chang, D.J., 1992. The p70 tumor necrosis factor receptor mediates cytotoxicity. Cell 70, 47.

Jacobs, M., Togbe, D., Fremond, C., Samarina, A., Allie, N., Botha, T., Carlos, D., Parida, S.K., Grivennikov, S., Nedospasov, S., Monteiro, A., Le Bert, M.,

Quesniaux, V., Ryffel, B., 2007. Tumor necrosis factor is critical to control tuberculosis infection. Microbes Infect. 9, 623.

Katayama, K., Wada, K., Miyoshi, H., Ohashi, K., Tachibana, M., Furuki, R., Mizuguchi, H., Hayakawa, T., Nakajima, A., Kadowaki, T., Tsutsumi, Y., Nakagawa, S., Kamisaki, Y., Mayumi, T., 2004. RNA interfering approach for clarifying the PPARgamma pathway using lentiviral vector expressing short hairpin RNA. FEBS Lett. 560, 178.

Krippner-Heidenreich, A., Tubing, F., Bryde, S., Willi, S., Zimmermann, G., Scheurich, P., 2002. Control of receptor-induced signaling complex formation by the kinetics of ligand/receptor interaction. J. Biol. Chem. 277, 44155.

Margolin, K., Aronson, F.R., Sznol, M., Atkins, M.B., Gucalp, R., Fisher, R.I., Sunderland, M., Doroshow, J.H., Ernest, M.L., Mier, J.W., et al., 1994. Phase II studies of recombinant human interleukin-4 in advanced renal cancer and malignant melanoma. J. Immunother. Emphas. Immunol. 15, 147.

Micheau, O., Tschopp, J., 2003. Induction of TNF receptor I-mediated apoptosis via two sequential signaling complexes. Cell 114, 181.

Miyoshi, H., Smith, K.A., Mosier, D.E., Verma, I.M., Torbett, B.E., 1999. Transduction of human CD34+ cells that mediate long-term engraftment of NOD/SCID mice by HIV vectors. Science 283, 682.

Nathan, D.M., Angus, P.W., Gibson, P.R., 2006. Hepatitis B and C virus infections and anti-tumor necrosis factor-alpha therapy: guidelines for clinical approach. J. Gastroenterol. Hepatol. 21, 1366.

Oh, P., Li, Y., Yu, J., Durr, E., Krasinska, K.M., Carver, L.A., Testa, J.E., Schnitzer, J.E., 2004. Subtractive proteomic mapping of the endothelial surface in lung and solid tumours for tissue-specific therapy. Nature 429, 629.

Schneeweiss, S., Setoguchi, S., Weinblatt, M.E., Katz, J.N., Avorn, J., Sax, P.E., Levin, R., Solomon, D.H., 2007. Anti-tumor necrosis factor alpha therapy and the risk of serious bacterial infections in elderly patients with rheumatoid arthritis. Arthritis Rheum. 56, 1754.

Shibata, H., Yoshioka, Y., Ikemizu, S., Kobayashi, K., Yamamoto, Y., Mukai, Y., Okamoto, T., Taniai, M., Kawamura, M., Abe, Y., Nakagawa, S., Hayakawa, T., Nagata, S., Yamagata, Y., Mayumi, T., Kamada, H., Tsutsumi, Y., 2004. Functionalization of tumor necrosis factor-alpha using phage display technique and PEGylation improves its antitumor therapeutic window. Clin. Cancer Res. 10, 8293.

Shibata, H., Yoshioka, Y., Ohkawa, A., Minowa, K., Mukai, Y., Abe, Y., Taniai, M., Nomura, T., Kayamuro, H., Nabeshi, H., Sugita, T., Imai, S., Nagano, K., Yoshikawa, T., Fujita, T., Nakagawa, S., Yamamoto, A., Ohta, T., Hayakawa, T., Mayumi, T., Vandenabeele, P., Aggarwal, B.B., Nakamura, T., Yamagata, Y., Tsunoda, S., Kamada, H., Tsutsumi, Y., 2008. Creation and X-ray structure analysis of the tumor necrosis factor receptor-1-selective mutant of a tumor necrosis factor-alpha antagonist. J. Biol. Chem. 283, 998.

Stanger, B.Z., Leder, P., Lee, T.H., Kim, E., Seed, B., 1995. RIP: a novel protein containing a death domain that interacts with Fas/APO-1 (CD95) in yeast and causes cell death. Cell 81, 513.

Szlosarek, P.W., Balkwill, F.R., 2003. Tumour necrosis factor alpha: a potential target for the therapy of solid tumours. Lancet Oncol. 4, 565.

Vandenabeele, P., Declercq, W., Beyaert, R., Fiers, W., 1995. Two tumour necrosis factor receptors: structure and function. Trends Cell Biol. 5, 392.

Vandenabeele, P., Declercq, W., Vercammen, D., Van de Craen, M., Grooten, J., Loetscher, H., Brockhaus, M., Lesslauer, W., Fiers, W., 1992. Functional characterization of the human tumor necrosis factor receptor p75 in a transfected rat/mouse T cell hybridoma. J. Exp. Med. 176, 1015.

Wajant, H., Pfizenmaier, K., Scheurich, P., 2003. Tumor necrosis factor signaling. Cell Death Differ. 10, 45.

Weiss, T., Grell, M., Siemienski, K., Muhlenbeck, F., Durkop, H., Pfizenmaier, K., Scheurich, P., Wajant, H., 1998. TNFR80-dependent enhancement of TNFR60-induced cell death is mediated by TNFR-associated factor 2 and is specific for TNFR60. J. Immunol. 161, 3136.

Xu, H., Sethi, J.K., Hotamisligil, G.S., 1999. Transmembrane tumor necrosis factor (TNF)-alpha inhibits adipocyte differentiation by selectively activating TNF receptor 1. J. Biol. Chem. 274, 26287.

Yamamoto, Y., Tsutsumi, Y., Yoshioka, Y., Nishibata, T., Kobayashi, K., Okamoto, T., Mukai, Y., Shimizu, T., Nakagawa, S., Nagata, S., Mayumi, T., 2003. Site-specific PEGylation of a lysine-deficient TNF-alpha with full bioactivity. Nat. Biotechnol. 21, 546.

Available online at www.sciencedirect.com
ScienceDirect
Biochimica et Biophysica Acta 1774 (2007) 1029–1035
Biochimica et Biophysica Acta
BBA
www.elsevier.com/locate/bbapap

Role of amino acid residue 90 in bioactivity and receptor binding capacity of tumor necrosis factor mutants

Hiroko Shibata [a,b], Haruhiko Kamada [a,c,*], Kyoko Kobayashi-Nishibata [b], Yasuo Yoshioka [c], Toshihide Nishibata [b], Yasuhiro Abe [a,b], Tetsuya Nomura [a,b], Hiromi Nabeshi [a], Kyoko Minowa [a], Yohei Mukai [a,b], Shinsaku Nakagawa [b], Tadanori Mayumi [d], Shin-ichi Tsunoda [a,c], Yasuo Tsutsumi [a,b,c]

[a] *National Institute of Biomedical Innovation, 7-6-8 Saito-Asagi, Ibaraki, Osaka 567-0085, Japan*
[b] *Department of Biotechnology and Therapeutics, Graduate School of Pharmaceutical Sciences, Osaka University, 1-6 Yamadaoka, Suita, Osaka 565-0871, Japan*
[c] *The Center for Advanced Medical Engineering and Informatics, Osaka University, 1-6 Yamadaoka, Suita, Osaka 565-0871, Japan*
[d] *Faculty of Pharmaceutical Sciences, Kobe-gakuin University, 518 Arise, Igawadani, Nishi-ku, Kobe 651-2180, Japan*

Received 12 March 2007; received in revised form 3 May 2007; accepted 3 May 2007
Available online 22 May 2007

Abstract

We have previously produced two bioactive lysine-deficient mutants of TNF-α (mutTNF-K90R,-K90P) and found that these mutants have bioactivity superior to wild-type TNF (wtTNF). Because these mutants contained same amino acid except for amino acid 90, it is unclear which amino acid residue is optimal for showing bioactivity. We speculated that this amino acid position was exchangeable, and this amino acid substitution enabled the creation of lysine-deficient mutants with enhanced bioactivity. Therefore, we produced mutTNF-K90R variants (mutTNF-R90X), in which R90 was replaced with other amino acids, to assay their bioactivities and investigated the importance of amino acid position 90. As a result, mutTNF-R90X that replaced R90 with lysine, arginine and proline were bioactive, while other mutants were not bioactive. Moreover, these three mutants showed bioactivity as good as or better than wtTNF. R90 replaced with lysine or arginine had especially superior binding affinities. These results suggest that the amino acid position 90 in TNF-α is important for TNF-α bioactivity and could be altered to improve its bioactivity to generate a "super-agonist".

Keywords: TNF; Mutant; Phage display; Lysine residue; TNF receptors; Structure

1. Introduction

TNF-α is an inflammatory cytokine able to mediate tumor regression in experimental and clinical cancers [1–3]. Attempts to use TNF-α for its cytotoxic property led to the development of several strategies that, in some cases, resulted in the use of TNF-α in clinical trials of tumor immuno-chemotherapy [4–6]. However, a frequent administration at high dose of TNF-α was required to obtain anti-tumor effect because of its poor stability and short half-lives, and resulted in severe side-effects [7]. Therefore, clinical application of TNF-α is still limited. More recently, some groups have reported positive results using melphalan in combination with TNF-α for patients with melanoma [8, 9]. These findings suggest that the enhanced anti-tumor effect of melphalan observed after the combination with TNF-α resulted from potentiation of the TNF-induced accumulation of melphalan into tumor accompanied by increased tumor vascular permeability [10]. The improved retention of TNF-α in the vascular space and the resultant decrease in transfer of TNF-α to normal tissues is expected to reduce the side effects of TNF-α therapy [11]. Thus, improving the circulation time of TNF-α may not only enhance its anti-tumor effects but also vascular permeability activity without increasing its side effects, resulting in longer bioavailability.

One of the most useful ways of enhancing the plasma half-lives of proteins is to conjugate them with polyethylene glycol (PEG) or other water-soluble polymeric modifiers [12–14]. The

* Corresponding author. National Institute of Biomedical Innovation, 7-6-8 Saito-Asagi, Ibaraki, Osaka 567-0085, Japan.
E-mail address: kamada@nibio.go.jp (H. Kamada).

1570-9639/$ - see front matter © 2007 Elsevier B.V. All rights reserved.
doi:10.1016/j.bbapap.2007.05.003

covalent conjugation of proteins with PEG (PEGylation) increases their molecular size and steric hindrance, both of which depend on the properties of the PEG attached to the protein. This prevents renal excretion and improves their proteolytic stability while decreasing their immunogenicity and hepatic uptake. We have also reported that optimal PEGylation of bioactive proteins could selectively improve their in vivo therapeutic potency and reduce side-effects [15, 16]. However, the PEGylation of proteins was mostly nonspecific and targeted lysine residues, some of which were in or near an active site. As a result, the PEGylation of proteins was accompanied by a significant loss of their specific activities in vitro [14, 17]. Thus, the clinical application of PEGylated proteins has been limited. To overcome the problems of PEGylation, we attempted to develop a novel strategy for site-specific mono-PEGylation of TNF-α to improve its antitumor potency in vivo [18, 19]. We produced bioactive lysine-deficient mutants of TNF-α (mutTNFs) from phage libraries expressing mutTNFs in which all of the six lysine residues were replaced with other amino acids. Among these mutant proteins, mutTNF-K90R and mutTNF-K90P have superior bioactivity, especially mutTNF-K90R, which has a 60-fold broader anti-tumor therapeutic window than wild-type TNF-α (wtTNF) [18].

Interestingly, these two mutTNFs were identical except for single amino acid changes at amino acid 90. Other lysine residues (amino acid 11, 65, 98, 112, 124) were replaced with alanine, serine, alanine, leucine, threonine respectively. Our previous study discussed the significance of R90 and P90 in the context of the TNF–TNF receptor structure. In the wtTNF structure, K90 forms a hydrogen bond with E135. This interaction likely stabilizes the loop structure containing residues 84 to 89, which is involved in receptor binding according to the model. In the mutTNF-K90R, arginine also is likely to be involved in hydrogen bonding with E135. The interaction may contribute to the stabilization of the loop structure. To confirm this speculation and clarify the importance of amino acid 90, it is necessary to create mutTNF-K90R variants (mutTNF-R90X) by replacing R90 with other amino acid in mutTNF-K90R, and validate their bioactivity, ability to form trimers, and binding affinity toward receptors. Moreover, the fact that only amino acid 90 substitutions were obtained highlights the importance of amino acid 90 as a key determinant between TNF-α and TNF receptor affinity and for its resulting level of bioactivity. This idea raises the possibility that mutTNFs with stronger bioactivity than mutTNF-K90R are created by the substitution of amino acid 90. Therefore, in this study, we evaluated the binding ability and bioactivity of mutTNF-R90X in order to examine the structural importance of the amino acid position 90 and to obtain mutTNFs with stronger bioactivity.

2. Materials and methods

2.1. Random amino-acid substitution of R90 in mutTNF-R90

The *Escherichia coli* library expressing mutTNF-R90 variants (mutTNF-R90Xs) in which R90 is replaced with other amino acids was constructed by the method as shown in Fig. 1. These mutTNF-R90Xs were also lysine-deficient except when X is lysine. pY02-mutTNF-R90 was used as a PCR template, and the arginine codon of mutTNF-R90 was replaced with the randomized sequence 'NNS (where N and S represent G/A/T/C or G/C, respectively) ' by two-step PCR using 4 primers. Oligo-1: 5′-cgG GCC AAG GCT GCC CCT CCA CCC ATG TGC TCC TCA CCC ACA CCA TCA GCC GCA TCG CCG TCT CCT ACC AGA CCN NS GTC AAC CTC CTC TCT GCC ATC-3′, Oligo-2 : 5′-GCC CAG ACT CGG CAA AGT CGA GAT AGT CGG GCC GAT TGA TCT CAG CGC T-3′, Oligo-3 : 5′-TGT ACC TTA TCT ACT CCC AGG TCC TCT TCT CGG GCC AAG GCT GCC CCT C-3′, Oligo-4 : 5′-GCC CAG ACT CGG CAA AGT CGA GAT AGT CGG GCC GAT TGA TCT CAG CGC T-3′. First PCR was carried out using Oligo-1 and -2. The PCR condition was cycled 30 times at 95 °C for 60 s, 57 °C for 60 s, and 68 °C for 60 s. PCR products (251 bp) were purified with QIAquick PCR purification Kits (QIAGEN, Valencia) and used as templates for second PCR. The second PCR was carried out using Oligo-

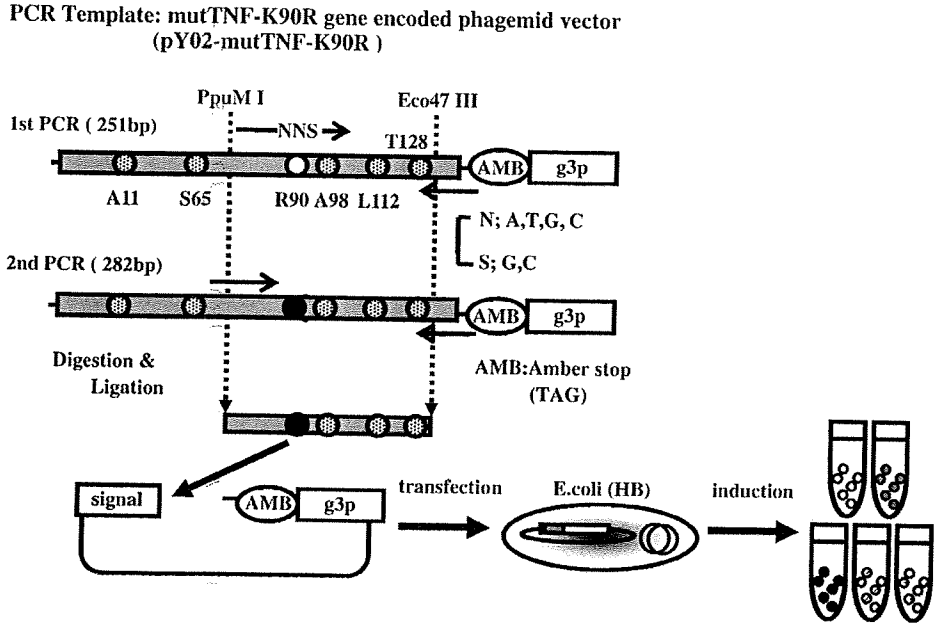

Fig. 1. Construction of mutTNF-R90X *E. coli* library.

3 and -4 under the same cycling conditions. Purified PCR products (283 bp) and pY02-mutTNF-K90R were digested with PpuM I and Eco47III. The resulting PCR products were inserted into pY02-mutTNF-K90R using T4 ligase (Roche Diagnostics, IN) at 16 °C for 16 h. Ligated DNAs were purified and introduced into *E. coli* HB2151 using a Bio-Rad Gene Pulser (Bio-Rad Laboratories, CA). The *E. coli* was then grown by culturing at 37 °C in LB agar medium with ampicillin (100 μg/mL) and glucose (2% w/v).

2.2. Preparation of E. coli culture supernatant

Colonies on LB agar medium were picked and grown by culturing at 37 °C in 2-YT medium with ampicillin (100 μg/mL) and glucose (2% w/v) until the OD_{600} of the culture medium reached 0.4. After centrifugation, supernatants were removed, and fresh 2-YT media with ampicillin (100 μg/mL) was added to *E. coli* pellets. After incubation for 6 h supernatants were collected and used for ELISA and bioassay.

2.3. TNF-α ELISA

Human TNF neutralizing monoclonal antibody (4 μg/mL, R&D systems, US) was coated onto Maxisorb immunoplates (NUNC, Denmark). After blocking, *E. coli* supernatant was then added into the plates and incubated at 37 °C for 2 h. The plates were washed three times with PBS and 0.05% Tween PBS and incubated with 200 ng/mL biotinylated anti-human TNF polyclonal antibody (R&D systems, US) at 37 °C for 1 h. After incubation, the plates were washed three times, and incubated with diluted avidin-HRP (Zymed Laboratories, Inc, US) at 37 °C for 1 h. After washing, TMB peroxidase substrate (MOSS, Inc. US) was added, and the absorbance was read at 450 nm / 650 nm using a micro plate reader.

2.4. Cytotoxicity assay

L-M cells, a cell line derived from L929 cells, were maintained in Eagle's Minimum Essential Medium (MEM, Sigma-Aldrich, Inc. Japan) with 1% bovine fetal serum and antibiotics. L-M cells treated with 1 μg/mL actinomycin D were seeded at 3×10^4 cells/well in 96 well plates, and cultured in the presence of *E. coli* supernatants or serially diluted TNFs. After incubation for 24 h, L-M cells were fixed by 25% glutaraldehyde and stained with 0.05% methylene blue for 15 min. After washing, 0.33 N HCl (100 μl) was added to each well, and the absorbance of released dye was measured at 655 nm /415 nm. Recombinant human TNF (R&D systems, US) was used as a standard.

In the case of HEp-2 cells, cells were maintained in RPMI 1640 medium (Sigma-Aldrich, Inc. Japan) with 10% bovine fetal serum, sodium pyruvate (1 mM), 2-mercaptoethanol (50 μM), and antibiotics. Cells were treated with 100 μg/mL cycloheximide, seeded at 4×10^4 cells/well, fixed after 18 h incubation, and used as described above.

2.5. Purification of recombinant proteins

Purification of recombinant proteins was described previously. Briefly, TNFs were produced in *E. coli* BL21(DE3). TNFs were recovered from inclusion bodies, which were washed in Triton X-100 and solubilized in 6 M guanidine–HCl, 0.1 M Tris–HCl, pH 8.0, and 2 mM EDTA. Solubilized protein (10 mg/mL) was reduced with 10 mg/mL dithioerythritol for 4 h at RT and refolded by 100-fold dilution in a refolding buffer, 100 mM Tris–HCl, 2 mM EDTA, 1 M arginine, and oxidized glutathione (551 mg/L). After dialysis with 20 mM Tris–HCl, pH 7.4, containing 100 mM urea, active trimeric proteins were purified by Q-Sepharose and MonoQ chromatography. Additionally, size-exclusion chromatography (Superose 12, GE Healthcare, England) was performed.

2.6. Surface plasmon resonance assay (BIAcore assay)

Human TNFR1 or TNFR2 Fc chimera (R&D systems, US) was diluted to 50 μg/mL in 10 mM sodium acetate buffer (pH 4.5) and immobilized to a CM3 sensor chip using an amine coupling kit (BIAcore, Sweden), which resulted in an increase of 4000–6000 resonance units (RU). During the association phase, mutTNFs or wtTNF diluted in running buffer (HBS-EP) at 26.1 nM, 8.7 nM or 2.9 nM were individually passed over the immobilized TNFRs at a flow rate of 20 μl/min. During the dissociation phase, HBS-EP buffer was applied to the sensor chip at a flow rate of 20 μl/min. Elution was carried out using 20 μl of 10 mM glycine–HCl. The data were analyzed globally with BIA EVALUATION 3.0 software (BIAcore®, Sweden) using a 1:1 binding model.

2.7. Induction of GM-CSF in PC60-hTNFR2 cells

PC60-hTNFR2, which is a cell line transfected with the human TNFR2, was kindly provided by Dr. Vandenabeele, and induction experiments were performed as previously described. PC60-hTNFR2 cells were cultured in RPMI-1640 supplemented with 10% bovine fetal serum, sodium pyruvate (1 mM), 2-ME (50 μM), and puromycin (3 μg/mL). Cells were seeded at 5×10^4 cells/well in 96 well plates with 2 ng/mL IL-1β (Peprotech, US) and serially diluted mutTNFs and wtTNF. After 24 h incubation, production of rat GM-CSF was quantified by ELISA according to the manufacturer's protocol (R&D systems, US).

3. Results

3.1. Phage library construction and bioactivity of mutTNF-R90X in culture supernatant of E. coli

In the first PCR step, DNA fragments (251 bp) in which the codon of R90 was replaced with an NNS sequence were synthesized. In the second PCR step, the first PCR product was extended to the PpuM I site. This second PCR product was digested with PpuM I and Eco47 III, and ligated with the phagemid vector pY02 to express mutTNF-R90X in culture supernatant of *E. coli*. We confirmed that R90 in clones was randomly replaced with other amino acids by sequence analysis (Fig. 1).

To screen the functional mutTNFs, the binding affinities of mutTNF-R90Xs for anti-human TNF-α neutralization antibody were measured using culture supernatant (Fig. 2). As a result, mutTNF-R90R, R90P, and R90K showed significant binding affinity for the anti-TNF-α neutralization antibody. Next, cytotoxicity of mutTNF-R90Xs against L-M cells was also evaluated using culture supernatant (Fig. 3). As a result, mutTNF-R90R, R90P, and R90K showed significant cytotoxi-

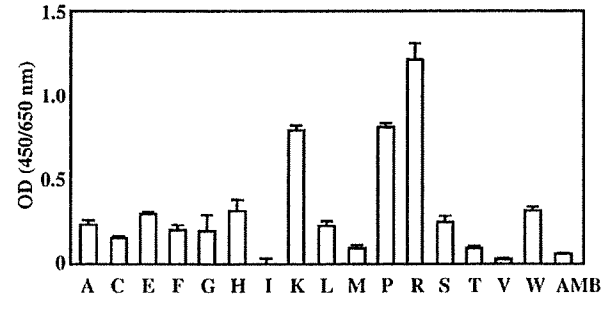

Fig. 2. Selection of clones by ELISA using anti-TNF neutralizing antibody. The reactivity of mutTNF-R90X with anti-TNF antibody was quantified by ELISA using culture supernatant of *E. coli* cells carrying the phagemid vector encoding mutTNF-R90X. Anti-TNF antibody was used as the capturing antibody, and bound mutTNF-R90X was detected with a biotinylated anti-TNF polyclonal antibody followed by addition of HRP-conjugated avidine and substrate reaction. Then the OD (450–655 nm) was measured. Each value represents the mean±SD.

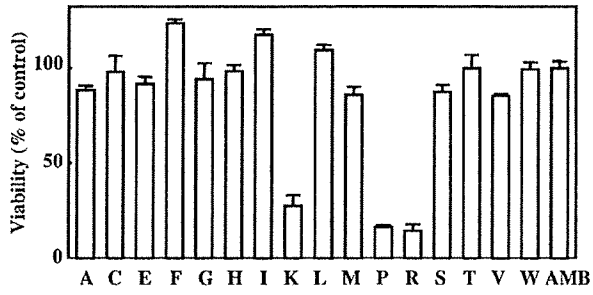

Fig. 3. Selection of clones by cytotoxicity assay using L-M cells. The cytotoxicity of mutTNF-R90X was assessed on L-M cells using culture supernatant of *E. coli* cells carrying the phagemid vector encoding mutTNF-R90X. L-M cells (3×10^4 cells/well) treated with actinomycin D were incubated with mutTNF-R90X for 24 h, and viabilities were assessed by methylene blue assay.

city to L-M cells. Other mutTNF-R90Xs have almost no affinity for anti-TNF-α antibody or show cytotoxicity. These results indicate that, as was expected, amino acid residue 90 should be lysine, arginine, or proline to retain its bioactivity and conformation.

3.2. Characterization of purified mutTNF-R90, P90, and K90

To assess their properties in detail, recombinant mutTNF-R90R, R90P, and R90K proteins were purified, and used in a binding analysis for TNF receptors, TNFR1 and TNFR2. As the result of gel filtration chromatography (GFC), the three mutTNF recombinant proteins exhibited the same retention time, indicating that they formed homotrimers (data not shown). Bioactivity of the three mutTNFs via mouse TNFR1 was confirmed using a cytotoxicity assay in L-M cells. As we reported previously, the cytotoxicity of mutTNF-R90P was almost the same as that of human wtTNF, while mutTNF-R90K was 3-fold higher and mutTNF-R90R was 5-fold higher (Fig. 4). Bioactivity of these mutTNFs via human TNFR1 was also assessed in HEp-2 cells. The cytotoxicity of mutTNF-R90P was the same as that of wtTNF. Interestingly, mutTNF-R90K and R90R exhibited 10-fold higher cytotoxicity than wtTNF (Fig. 5). Finally, bioactivity via human TNFR2 was assessed on GM-CSF production from PC60-hTNFR2 cells (human TNFR2 transfected PC60 cells). All three mutTNFs showed 2-fold higher bioactivity via TNFR2 than wtTNF (Fig. 6). These results indicate that mutTNF-R90R and R90K can stimulate TNFR1 more selectively than wtTNF.

3.3. Kinetics of mutTNFs on TNFR1 and TNFR2 affinity

The increase in affinity for TNF receptors may be one of the factors that contribute to the bioactivity enhancement. Therefore, we measured the affinities of mutTNFs for TNFR1 and TNFR2 using surface plasmon resonance (BIAcore). By comparison of the dissociation constants (KD) of mutTNFs against TNFR1, the affinities of mutTNF-R90K and R90P were 2 to 3-fold higher than wtTNF (Table 1). The affinity of mutTNF-R90P, however, was half that of wtTNF. Thus, the

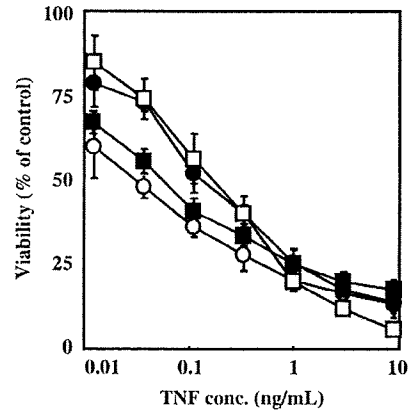

	EC50 (ng/mL)
□ wtTNF	0.17
■ mutTNF-R90K	0.05
○ mutTNF-R90R	0.03
● mutTNF-R90P	0.14

Fig. 4. Cytotoxicity of mutTNFs against L-M cells. The bioactivity of mutTNF via mouse TNFR1 was measured by the cytotoxicity assay against L-M cells in the presence of actinomycin D. Each value represents the mean±SD. The EC_{50} shows the concentration of TNF required to inhibit L-M cell viability by 50%.

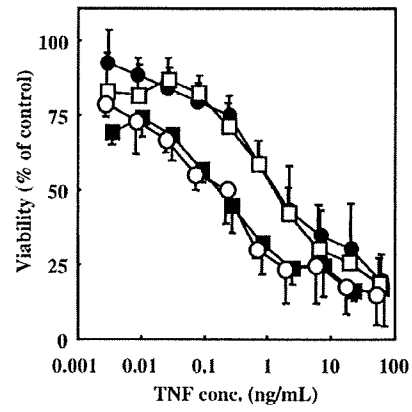

	EC50 (ng/mL)
□ wtTNF	1.30
■ mutTNF-R90K	0.17
○ mutTNF-R90R	0.15
● mutTNF-R90P	1.40

Fig. 5. Cytotoxicity of mutTNFs against HEp-2 cells. The bioactivity of mutTNF via human TNFR1 was measured by a cytotoxicity assay against HEp-2 cells in the presence of cycloheximide. HEp-2 cells (4×10^4 cells/well) were incubated with mutTNFs for 18 h, and their viabilities were assessed by methylene blue assay. Each value represents the mean±SD. The EC_{50} shows the concentration of TNF required to inhibit HEp-2 cell viability by 50%.

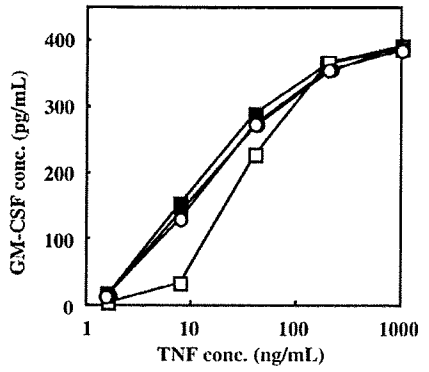

		EC50 (ng/mL)
□	wtTNF	41.5
■	mutTNF-K90K	16.3
○	mutTNF-K90R	19.9
●	mutTNF-K90P	19.8

Fig. 6. Induction of GM-CSF by mutTNFs. PC60 cells transfected human TNFR2 were incubated with mutTNFs and IL-1β (2 ng/mL). After 24 h, TNFR2-mediated induction of GM-CSF was assayed by ELISA. Each value represents the mean±SD. The EC_{50} is given as the concentration of TNF-α required to induce secretion of 200 pg/mL GM-CSF.

lower bioactivity of mutTNF-R90P via TNFR1 may be due to weaker affinity for TNFR1. On the other hand, affinities of the three mutTNFs for TNFR2 were 1.2- to 1.5-fold higher than that of wtTNF (Table 2). These results suggest that replacement of amino acid residue 90 in mutTNF does not affect the affinity for TNFR2, while arginine or lysine substitution at amino acid residue 90 is better than proline for TNFR1 binding.

4. Discussion

Although systemic administration of TNF-α is limited due to its severe side effects, TNF exerts beneficial anti-tumor effects as an enhancer of tumor vascular permeability in combination cancer chemotherapy [8–10]. Therefore, the creation of an artificial mutTNF with remarkable bioactivity and in vivo stability will be important to generate a more effective cancer chemotherapy. We have previously created lysine-deficient mutTNFs, mutTNF-R90 and P90, which showed high bioactivity and in vivo stability and are suitable for site-specific mono-PEGylation [18]. We have also reported that these lysine-deficient mutTNFs show the same or higher bioactivities than wtTNF and that mono-PEGylated mutTNFs exhibit increased anti-tumor therapeutic potential. In this study, we attempted to create a new mutTNF that has more bioactivity and a tighter binding affinity when compared to mutTNF-R90 and P90. We also evaluated the role of amino acid residue 90 in bioactivity and receptor binding capacity.

Table 1
Kinetic parameters of mutant TNF-αs (TNF receptor 1)

	Ka[a] (10^5)(1/Ms)	Kd[b] (10^{-3})(1/s)	KD[c] (10^{-9})(M)	Relative[d] (%)
Human wtTNF	5.4	1.2	2.3	100
mutTNF-R90K	13.4	1.1	0.8	285
mutTNF-R90P	4.0	2.1	5.2	44
mutTNF-R90R	12.1	1.4	1.2	191

Kinetic parameters were determined from equilibrium binding using BIA evaluation 3.0 program.
[a] Association rate constant.
[b] Dissociation rate constant.
[c] Equilibrium dissociation constant.
[d] Relative values for the KD were calculated from the KD (mutants)/KD (wtTNF)×100.

Table 2
Kinetic parameters of mutant TNF-αs (TNF receptor 2)

	Ka[a] (10^6) (1/Ms)	Kd[b] (10^{-4}) (1/s)	KD[c] (10^{-10}) (M)	Relative[d] (%)
Human wtTNF	3.7	10.1	2.7	100
mutTNF-R90K	5.1	10.7	2.1	129
mutTNF-R90P	5.1	11.3	2.2	122
mutTNF-R90R	5.2	9.4	1.8	148

Kinetic parameters were determined from equilibrium binding using BIA evaluation 3.0 program.
[a] Association rate constant.
[b] Dissociation rate constant.
[c] Equilibrium dissociation constant.
[d] Relative values for the KD were calculated from the KD (mutants)/KD (wtTNF)×100.

We constructed a phage library that expresses mutTNF-R90 variants in which R90 is replaced with other amino acids and measured their affinities for anti-TNF-α and their bioactivities using culture supernatant of *E. coli*. Only mutTNF-R90X in which amino acid residue 90 was replaced with lysine, arginine, or proline exhibited affinity for anti-TNF-α and bioactivity. Therefore, it is suggested that proline, arginine and lysine at position 90 are important to retain the bioactivity of TNF-α. As described previously, K90 in wtTNF forms a hydrogen bond with E135 in TNFR1 and contributes to stabilizing the loop structure that contains residues 84 to 89, which is the receptor binding region. In the mutTNF-R90R, R90 also likely forms a hydrogen bond with E135 and perhaps contributes to stabilizing the loop structure. The basic amino acid substitution mutTNF-R90H had no bioactivity nor binding affinity. These results suggest that general replacement of R90 with a basic amino acid is not always essential for bioactivity and binding affinity to the TNF receptor. Moreover, the steric hindrance of an amino acid residue is as important as electric charge.

Lysine residues in proteins are generally believed to be important amino acids for retaining three-dimensional structure and for receptor affinity and bioactivity. In the case of TNF-α, X-ray structure analysis revealed that K11 and K98 are important for retaining protein structure and homotrimerization [20]. However, the importance of other lysine residues (K65, 90, 112, 128) has not been discussed. The only report with regard to K90 demonstrated that replacement of K90 with alanine reduced the bioactivity to half of wtTNF [21]. Our results indicate that amino acid position 90 of TNF-α is important for homotrimer formation and bioactivity.

We measured the bioactivities and affinities of mutTNF-R90R, R90K and R90P for TNF receptors. mutTNF-R90R and mutTNF-R90K demonstrated 10-fold higher cytotoxicity levels in HEp-2 cells than wtTNF. The cytotoxicity level of mutTNF-R90P was almost the same as wtTNF. Indeed, affinities of mutTNF-R90R and -R90K for TNFR1 were 2 to 3-fold higher than wtTNF, while that of mutTNF-R90P was half that of wtTNF. Thus R90 and K90 contribute to the stable formation of the TNF/TNFR1 complex, and this may be one of the factors causing increased bioactivity. On the other hand, TNFR2-dependent bioactivities of the three mutants almost doubled that of wtTNF. Affinities of the three mutants for TNFR2 were also 1.2 to 1.5 stronger that that of wtTNF. These results indicate that arginine or lysine in amino acid position 90 is necessary for mutTNFs to obtain superior bioactivity and affinity for TNFR1, but less so for TNFR2. A previous study showed that the loop structure mutant TNF S86T had TNFR1-selectivity [22]. The interaction site of this loop structure with TNFR1 is predicted to be different than with TNFR2. The lower affinity of mutTNF-R90P for TNFR1 (as compared with mutTNF-R90K or-R90R) is thought to be caused by the difference in loop structure stabilization. The hydrogen bond formed between the basic amino acid (K90 or R90) and E135 creates a more stable loop than one stabilized by the hydrophobic bond between P90 and L83. Interestingly, in the lysine-deficient mutTNF that we previously created, K90 was replaced with proline [19]. This result indicates that the loop structure formed by the hydrophobic interaction of P90 with L83 is very important to protein folding and homotrimer formation.

In this study, we created mutTNFs that substitute other amino acids in the K90 position and evaluated their bioactivities and binding affinities. The determination of the functional domain of TNF has been attempted by creating mutant TNFs like these, however, there are few reports that detailed the role of one amino acid in TNF-α. Our data demonstrate that amino acid position 90 is important for TNF bioactivity and that replacement with other amino acids will be an effective strategy to increase the bioactivity of TNF-α. In the near future, the accumulation of information about the structure–activity relationship of TNF-α using mutant TNFs will enable the generation of a super-agonist that has optimized bioactivity.

Acknowledgements

This study was supported by a Grant-in-Aid for Scientific Research (No. 17016084 and 17689008, 17790135, 18015055, 18659047) from the Ministry of Education, Culture, Sports, Science and Technology of Japan, a Health and Labor Sciences Research Grant from the Ministry of Health, Labor and Welfare of Japan, Takeda Scientific Foundation and Research Fellowships for Young Scientists.

References

[1] E.A. Carswell, L.J. Old, R.L. Kassel, S. Green, N. Fiore, B. Williamson, An endotoxin-induced serum factor that causes necrosis of tumors, Proc. Natl. Acad. Sci. U. S. A. 72 (1975) 3666–3670.

[2] E.A. Havell, W. Fiers, R.J. North, The antitumor function of tumor necrosis factor (TNF), I. Therapeutic action of TNF against an established murine sarcoma is indirect, immunologically dependent, and limited by severe toxicity, J. Exp. Med. 167 (1988) 1067–1085.

[3] L. Helson, C. Helson, S. Green, Effects of murine tumor necrosis factor on heterotransplanted human tumors, Exp. Cell Biol. 47 (1979) 53–60.

[4] W.L. Furman, D. Strother, K. McClain, B. Bell, B. Leventhal, C.B. Pratt, Phase I clinical trial of recombinant human tumor necrosis factor in children with refractory solid tumors: a Pediatric Oncology Group study, J. Clin. Oncol. 11 (1993) 2205–2210.

[5] K. Kimura, T. Taguchi, I. Urushizaki, R. Ohno, O. Abe, H. Furue, T. Hattori, H. Ichihashi, K. Inoguchi, H. Majima, Phase I study of recombinant human tumor necrosis factor, Cancer Chemother. Pharmacol. 20 (1987) 223–239.

[6] T. Moritz, N. Niederle, J. Baumann, D. May, E. Kurschel, R. Osieka, J. Kempeni, E. Schlick, C.G. Schmidt, Phase I study of recombinant human tumor necrosis factor alpha in advanced malignant disease, Cancer Immunol. Immunother. 29 (1989) 144–150.

[7] J. Skillings, R. Wierzbicki, E. Eisenhauer, P. Venner, F. Letendre, D. Stewart, B. Weinerman, A phase II study of recombinant tumor necrosis factor in renal cell carcinoma: a study of the National Cancer Institute of Canada Clinical Trials Group, J. Immunother. 11 (1992) 67–70.

[8] A.M. Eggermont, H. Schraffordt Koops, D. Lienard, B.B. Kroon, A.N. van Geel, H.J. Hoekstra, F.J. Lejeune, Isolated limb perfusion with high-dose tumor necrosis factor-alpha in combination with interferon-gamma and melphalan for nonresectable extremity soft tissue sarcomas: a multicenter trial, J. Clin. Oncol. 14 (1996) 2653–2665.

[9] D. Lienard, P. Ewalenko, J.J. Delmotte, N. Renard, F.J. Lejeune, High-dose recombinant tumor necrosis factor alpha in combination with interferon gamma and melphalan in isolation perfusion of the limbs for melanoma and sarcoma, J. Clin. Oncol. 10 (1992) 52–60.

[10] F.J. Lejeune, Clinical use of TNF revisited: improving penetration of anti-cancer agents by increasing vascular permeability, J. Clin. Invest. 110 (2002) 433–435.

[11] F.J. Lejeune, C. Ruegg, D. Lienard, Clinical applications of TNF-alpha in cancer, Curr. Opin. Immunol. 10 (1998) 573–580.

[12] P. Bailon, A. Palleroni, C.A. Schaffer, C.L. Spence, W.J. Fung, J.E. Porter, G.K. Ehrlich, W. Pan, Z.X. Xu, M.W. Modi, A. Farid, W. Berthold, M. Graves, Rational design of a potent, long-lasting form of interferon: a 40 kDa branched polyethylene glycol-conjugated interferon alpha-2a for the treatment of hepatitis C, Bioconjug. Chem. 12 (2001) 195–202.

[13] H. Kamada, Y. Tsutsumi, K. Sato-Kamada, Y. Yamamoto, Y. Yoshioka, T. Okamoto, S. Nakagawa, S. Nagata, T. Mayumi, Synthesis of a poly (vinylpyrrolidone-co-dimethyl maleic anhydride) co-polymer and its application for renal drug targeting, Nat. Biotechnol. 21 (2003) 399–404.

[14] H. Kamada, Y. Tsutsumi, Y. Yamamoto, T. Kihira, Y. Kaneda, Y. Mu, H. Kodaira, S.I. Tsunoda, S. Nakagawa, T. Mayumi, Antitumor activity of tumor necrosis factor-alpha conjugated with polyvinylpyrrolidone on solid tumors in mice, Cancer Res. 60 (2000) 6416–6420.

[15] Y. Kaneda, Y. Yamamoto, H. Kamada, S. Tsunoda, Y. Tsutsumi, T. Hirano, T. Mayumi, Antitumor activity of tumor necrosis factor alpha conjugated with divinyl ether and maleic anhydride copolymer on solid tumors in mice, Cancer Res. 58 (1998) 290–295.

[16] Y. Tsutsumi, S. Tsunoda, H. Kamada, T. Kihira, Y. Kaneda, Y. Ohsugi, T. Mayumi, PEGylation of interleukin-6 effectively increases its thrombopoietic potency, Thromb. Haemost. 77 (1997) 168–173.

[17] S.P. Monkarsh, Y. Ma, A. Aglione, P. Bailon, D. Ciolek, B. DeBarbieri, M.C. Graves, K. Hollfelder, H. Michel, A. Palleroni, J.E. Porter, E. Russoman, S. Roy, Y.C. Pan, Positional isomers of monopegylated interferon alpha-2a: isolation, characterization, and biological activity, Anal. Biochem. 247 (1997) 434–440.

[18] H. Shibata, Y. Yoshioka, S. Ikemizu, K. Kobayashi, Y. Yamamoto, Y. Mukai, T. Okamoto, M. Taniai, M. Kawamura, Y. Abe, S. Nakagawa, T. Hayakawa, S. Nagata, Y. Yamagata, T. Mayumi, H. Kamada, Y. Tsutsumi, Functionalization of tumor necrosis factor-alpha using phage display technique and PEGylation improves its antitumor therapeutic window, Clin. Cancer Res. 10 (2004) 8293–8300.

[19] Y. Yamamoto, Y. Tsutsumi, Y. Yoshioka, T. Nishibata, K. Kobayashi, T.

Okamoto, Y. Mukai, T. Shimizu, S. Nakagawa, S. Nagata, T. Mayumi, Site-specific PEGylation of a lysine-deficient TNF-alpha with full bioactivity, Nat. Biotechnol. 21 (2003) 546–552.
[20] M.J. Eck, S.R. Sprang, The structure of tumor necrosis factor-alpha at 2.6 A resolution. Implications for receptor binding, J. Biol. Chem. 264 (1989) 17595–17605.
[21] J. Yamagishi, H. Kawashima, N. Matsuo, M. Ohue, M. Yamayoshi, T. Fukui, H. Kotani, R. Furuta, K. Nakano, M. Yamada, Mutational analysis of structure–activity relationships in human tumor necrosis factor-alpha, Protein Eng. 3 (1990) 713–719.
[22] H. Loetscher, D. Stueber, D. Banner, F. Mackay, W. Lesslauer, Human tumor necrosis factor alpha (TNF alpha) mutants with exclusive specificity for the 55-kDa or 75-kDa TNF receptors, J. Biol. Chem. 268 (1993) 26350–26357.

Biomaterials 30 (2009) 5869–5876

Contents lists available at ScienceDirect

Biomaterials

journal homepage: www.elsevier.com/locate/biomaterials

The use of a mutant TNF-α as a vaccine adjuvant for the induction of mucosal immune responses

Hiroyuki Kayamuro [a,b,1], Yasuhiro Abe [a,1], Yasuo Yoshioka [a,c,1], Kazufumi Katayama [b,d], Tetsuya Nomura [a,b], Tokuyuki Yoshida [a,b], Kohei Yamashita [a,b], Tomoaki Yoshikawa [a,b], Yuichi Kawai [e], Tadanori Mayumi [e], Takachika Hiroi [d], Norio Itoh [b], Kazuya Nagano [a], Haruhiko Kamada [a,c], Shin-ichi Tsunoda [a,c,*], Yasuo Tsutsumi [a,b,c]

[a] Laboratory of Pharmaceutical Proteomics, National Institute of Biomedical Innovation (NiBio), 7-6-8 Saito-Asagi, Ibaraki, Osaka 567-0085, Japan
[b] Graduate School of Pharmaceutical Sciences, Osaka University, 1-6, Yamadaoka, Suita, Osaka 565-0871, Japan
[c] The Center for Advanced Medical Engineering and Informatics, Osaka University, 1-6, Yamadaoka, Suita, Osaka 565-0871, Japan
[d] Department of Allergy and Immunology, The Tokyo Metropolitan Institute of Medical Science, 3-18-22, Honkomagome, Bunkyo-ku, Tokyo 113-8613, Japan
[e] Faculty of Pharmaceutical Sciences, Kobe-Gakuin University, 1-1-3, Minatojima, Chuo-ku, Kobe 650-8586, Japan

ARTICLE INFO

Article history:
Received 19 May 2009
Accepted 6 July 2009
Available online 30 July 2009

Keywords:
Bioactivity
Cytokine
Mucosa
Immunomodulation

ABSTRACT

Safe and potent adjuvants are required in order to establish effective mucosal vaccines. Cytokines are promising adjuvants because they are human-derived safe biomaterial and display immune-modulating functions. We have created a mutant tumor necrosis factor-α (TNF-α), mTNF-K90R, that exhibits high bioactivity and resistance to proteases. Here, we examined the potential of mTNF-K90R as a mucosal adjuvant. Initially, we showed that intranasal co-administration of mTNF-K90R with ovalbumin (OVA) potently produced OVA-specific Immunoglobulin (Ig) G antibodies (Abs) in serum and IgA Abs both at local and distal mucosal sites compared to co-administration with wild-type TNF-α. The OVA-specific immune response was characterized by high levels of serum IgG1 and increased production of interleukin-4 (IL-4), IL-5 and IL-10 from splenocytes of immunized mice, suggesting a Th2 response. Furthermore, intranasal immunization with an antigen from influenza virus plus mTNF-K90R exhibited mucosal adjuvant activity for induction of both systemic and mucosal immune responses. Importantly, histopathological examination of the nasal tissue of mTNF-K90R treated mice detected no signs of toxicity. These findings suggest that mTNF-K90R is safe and effective mucosal adjuvant and this system may have potential application as a universal mucosal adjuvant system for mucosal vaccines improving the immune response to a variety of viral antigens.

1. Introduction

Mucosal immunity forms the first line of defense against various infectious diseases. The majority of emerging and re-emerging pathogens, including *Vibrio cholerae*, pathogenic *Escherichia coli*, HIV or influenza virus, invade and infect *via* the mucosal surfaces of the host gastrointestinal, respiratory and/or genitourinary tracts [1,2]. An important aspect of the immune response at mucosal surfaces is the production of polymeric immunoglobulin (Ig) A antibodies (Abs), as well as their transport across the epithelium and release as secretory IgA [3]. Because this IgA response represents the major mechanism for defense against viral and bacterial infections, recent efforts have been focused on the development of vaccines that are capable of inducing IgA production as well as cytotoxic T cell activation efficiently in mucosal tissues.

Mucosal vaccines administered either orally or nasally have been shown to be effective in inducing antigen-specific immune responses at both systemic and mucosal compartments [4,5]. Because of this two-layered protective immunity, mucosal vaccines are thought to be an ideal strategy for combating both emerging and re-emerging infectious diseases. However the mucosal antigen-specific immune response is weak because most protein antigens, such as non-living macromolecules or protein-subunit antigens, can evoke only a weak or undetectable adaptive immune response when they are applied mucosally [6]. Therefore, one strategy to overcome the weakness of the immune response is a co-administration of mucosal adjuvant

* Corresponding author. Laboratory of Pharmaceutical Proteomics, National Institute of Biomedical Innovation (NiBio), 7-6-8 Saito-Asagi, Ibaraki, Osaka 567-0085, Japan. Tel.: +81 72 641 9811; fax: +81 72 641 9817.
E-mail address: tsunoda@nibio.go.jp (S.-i. Tsunoda).
[1] These authors contributed equally to the work.

0142-9612/$ – see front matter © 2009 Elsevier Ltd. All rights reserved.
doi:10.1016/j.biomaterials.2009.07.009

with the vaccine antigen [4]. Unfortunately, the development of safe and effective mucosal adjuvant has proved to be challenging. As a potent mucosal vaccine adjuvant, cholera toxin (CT) or heat liable toxin have been used in experimental studies. However, the watery diarrhea induced by the administration of these toxins precludes their use as oral adjuvants in humans [7]. In addition, recent reports show that a human vaccine containing inactivated influenza and heat liable toxin as a mucosal adjuvant results in a very high incidence of Bell's palsy [8]. Therefore, development of novel mucosal vaccine adjuvants with high efficacy and safety is urgently required for clinical applications.

Cytokines are promising candidate adjuvants because they are human-derived and able to enhance the primary and memory immune responses sufficiently for protection against various infections [9–11]. One of the most important cytokines of adaptive and innate immune response is tumor necrosis factor-α (TNF-α), a proinflammatory cytokine primarily produced by T cells and macrophages [12]. TNF-α has been reported to affect certain phases of the immune process, including innate immune activation, dendritic cells (DC) maturation/recruitment, T cell activation, or pathogen clearance [13]. Indeed many reports have shown that TNF-α exerts adjuvant activities against viral infection in various model systems [14–16]. Therefore the application of TNF-α in the development of a vaccine adjuvant has been anticipated for some time. However the application of TNF-α as a mucosal vaccine adjuvant has not been reported because TNF-α administered by mucosal routes is rapidly degraded at the mucosal surface. Therefore, the maximum adjuvant effects of TNF-α are quite limited in the mucosal environment.

Previously, we have produced a bioactive lysine-deficient mutant TNF-αs from a phage library expressing mutant TNF-αs in which all of the lysine residues that act as a site of trypsin-type protease recognition were replaced with other amino acids [17–19]. Lysine-deficient mutant TNF-αs were more resistant to proteolytic cleavage than wild-type TNF-α (wTNF-α) due to the lack of lysine residues. Furthermore we demonstrated that the mTNF-K90R, one of the lysine-deficient mutant TNF-αs, showed 6-fold stronger *in vitro* bioactivity and 13-fold stronger *in vivo* bioactivity compared with wTNF-α [18].

In this study, to develop effective and safe cytokine-based mucosal vaccine adjuvants, we examined the potential of mTNF-K90R as a nasal vaccine adjuvant. We demonstrate that intranasal administration of vaccine antigen with mTNF-K90R as an adjuvant induces a strong antigen-specific systemic IgG and mucosal IgA response. In addition, the safety of mTNF-K90R was confirmed by pathological examination. These results suggest that mTNF-K90R is an attractive mucosal vaccine adjuvant for clinical application.

2. Materials and methods

2.1. Recombinant TNF-αs

wTNF-α and mTNF-K90R were prepared in house as described previously [18]. Endotoxin level was quantified using a Limulus amebocyte lysate assay kit (QCL-1000, BioWhittaker, Walkersville, MD). The endotoxin content of purified TNF-α and its mutant was <0.02 EU μg^{-1} protein.

2.2. Mice and immunization protocols

Female BALB/c mice were purchased from Nippon SLC (Kyoto, Japan) and used at 6–8 weeks of age. All of the animal experimental procedures were performed in accordance with the institutional ethical guidelines for animal experiments. Mice were intranasally immunized with a 20 μl aliquot (10 μl per nostril) containing 100 μg of ovalbumin (OVA; Sigma Chemical Co., St. Louis, MO) as antigen and 1 or 5 μg of wTNF-α or mTNF-K90R on days 0, 7 and 14. As positive control, mice were intranasally immunized with the same volume containing 100 μg of OVA and 1 μg cholera toxin B subunit (CTB; List Biological Laboratories, Campbell, CA) on days 0, 7 and 14. In the influenza virus studies, 1 μg baculovirus-expressed recombinant hemagglutinin (HA) derived from New Cal/99 virus (Protein Sciences, Meriden, CT), was immunized with 1 μg CTB or 5 μg mTNF-K90R on days 0, 7 and 14.

2.3. Sample collection

One week after the final immunization, plasma and mucosal secretions (nasal washes, saliva, vaginal washes and fecal extracts) were collected to assess antigen-specific Ab responses. Nasal and vaginal washes were collected by gentle flushing of the nasal passage or vaginal canal with 200 μl or 100 μl of sterile phosphate buffered saline (PBS), respectively. Fecal pellets (100 mg) were suspended in 1 ml of PBS and then vortexed for 30 min. The samples were centrifuged at 15 000g for 20 min and the supernatants were then collected as fecal extracts. Secreted saliva was collected from mice intraperitoneally injected with 0.2 mg of pilocarpine–HCl (Wako Pure Chemical Industries, Osaka, Japan).

2.4. Detection of antigen-specific Ab responses by enzyme-linked immunosorbent assay (ELISA)

Antigen-specific Ab levels in plasma, nasal washes, saliva, vaginal washes and fecal extracts were determined by ELISA. ELISA plates (Maxisorp, type 96F; Nalge Nunc International, Tokyo, Japan) were coated with 10 μg ml^{-1} OVA or 2 μg ml^{-1} HA in 0.1 M carbonate buffer and incubated overnight at 4 °C. The plates were incubated with blocking solution (Block Ace; Dainippon Sumitomo Pharmaceuticals, Osaka, Japan) at 37 °C for 2 h, and serum or mucosal secretion dilutions were added to the antigen-coated plates. After incubation at 37 °C for 2 h, the coated plates were washed with PBS–Tween 20 and incubated with a horseradish peroxidase-conjugated goat anti-mouse IgG solution or a biotin-conjugated goat anti-mouse IgA detection Ab (Southern Biotechnology Associates, Birmingham, AL) solution at 37 °C for 2 h, respectively. For detection of IgA, the plates were washed with PBS–Tween 20 and then incubated with the horseradish peroxidase-coupled streptavidin (Zymed Laboratories, South San Francisco, CA) for 1 h at RT. After incubation, the color reaction was developed with tetramethylbenzidine (MOSS, Inc. Pasadena, MD), stopped with 2 N H_2SO_4, and measured by $OD_{450-655}$ on a microplate reader.

2.5. Isolation of splenocytes

Spleens were aseptically removed and placed in RPMI 1640 (Wako Pure Chemical Industries, Osaka, Japan) supplemented with 10% fetal bovine serum, 50 μM 2-mercaptoethanol and 1% antibiotic cocktail (Nacalai tesque, Kyoto, Japan). Single-cell suspension of splenocytes was treated with ammonium chloride to lyse the red blood cells, washed, counted, and suspended in RPMI supplemented with 10% fetal bovine serum, 50 μM 2-mercaptoethanol, 1% antibiotic cocktail, 10 ml L^{-1} of a 100× nonessential amino acids solution (NEAA; Gibco-BRL), 1 mM sodium pyruvate, and 10 mM HEPES to a final concentration of 1×10^7 cells ml^{-1}.

2.6. Antigen-specific cytokine responses

Antigen-specific cytokine responses were evaluated by culturing the splenocytes (5×10^6 cells $well^{-1}$) stimulated with OVA (1 mg ml^{-1}) *in vitro*. Cells were incubated at 37 °C for 24 h (interferon-γ (IFN-γ) enzyme-linked immunospot (ELISPOT) assay), 48 h (IL-4 ELISPOT assay) or 72 h (multiplex cytokine assay).

2.7. Multiplex cytokine assay

Culture supernatants from *in vitro* unstimulated and OVA-stimulated cells were analyzed by the Bio-Plex Multiplex Cytokine Assay (Bio-Rad Laboratories, Hercules, CA) according to the manufacturer's instructions. The assay was read on a Luminex 100 (Austin, TX), and analyzed using Bio-Plex Manager software. The mean concentration of cytokines in supernatants from OVA-stimulated cells over the unstimulated background was then calculated.

2.8. Cytokine ELISPOT assay

An ELISPOT assay was performed to detect IFN-γ and IL-4 producing cells. After 24 h (IFN-γ) or 48 h (IL-4) incubation at 37 °C, the plate was washed, and the IFN-γ and IL-4 producing cells were measured by an ELISPOT assay kit (BD Biosciences), according to the manufacturer's instructions.

2.9. Fluorescence microscopy

BALB/c mice were administered intranasally with fluorescent isothiocyanate (FITC) labeled OVA (FITC-OVA; Molecular Probes–Invitrogen, Eugene, OR) at 50 μg $mouse^{-1}$ with or without mTNF-K90R (5 μg $mouse^{-1}$). After 15 min, the heads of the anesthetized mice were severed from the body. The heads were placed in fixative solution, and embedded in OCT compound (Sakura FineTek Japan Co. Ltd., Tokyo, Japan) and frozen tissue sections were prepared. FITC-OVA was observed under fluorescence microscopy (×20).

2.10. Histopathological analysis

For three times immunization protocol, BALB/c mice were immunized with OVA with or without mTNF-K90R at a dose of 1 μg, 5 μg or 25 μg on days 0, 7 and 14.